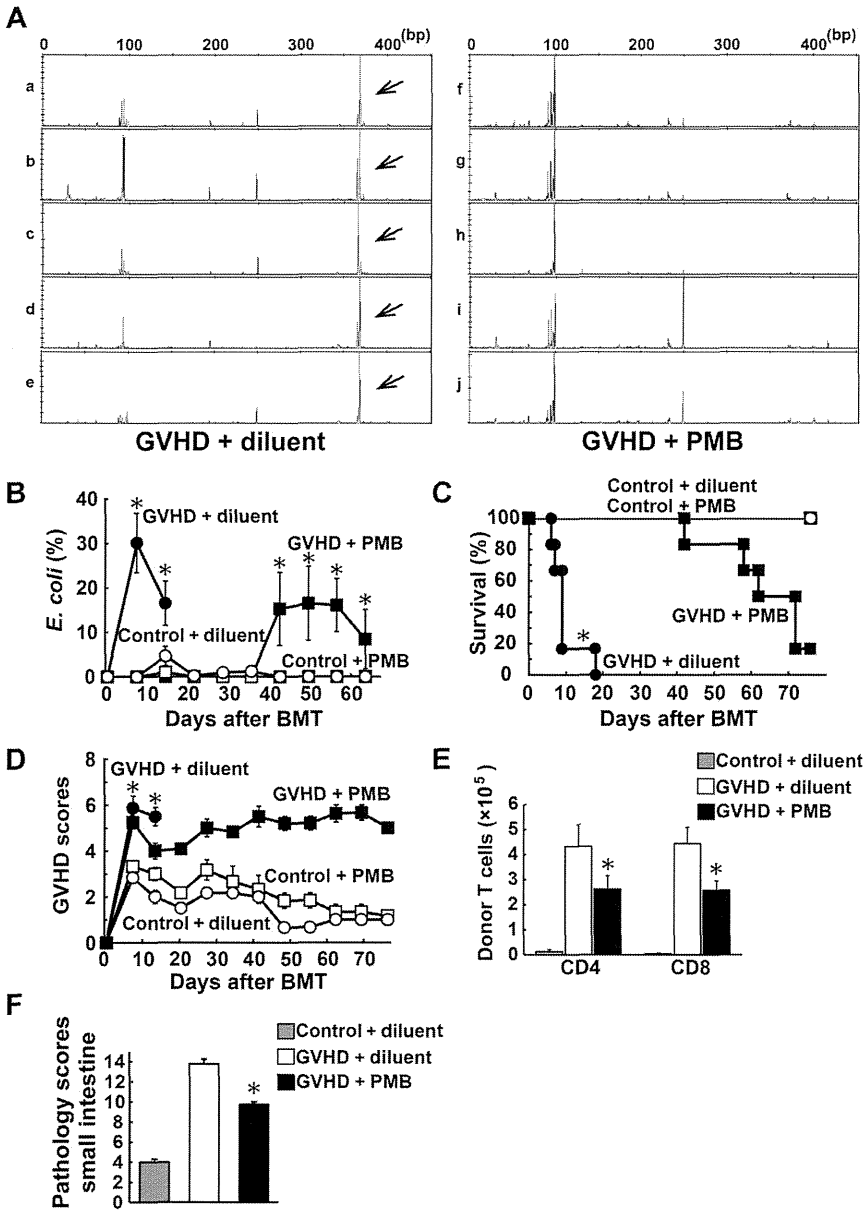

Figure 7. Oral administration of polymyxin B ameliorated GVHD. Lethally irradiated B6D2F1 mice were transplanted with 5×10^6 TCD BM without or with 2×10^6 T cells from B6 or B6-Ly5.1 (CD45.1$^+$) donors. Polymyxin B (PMB; 100 mg/kg) or diluent was administered by daily oral gavage from day −4 until day 28 after BMT. (A) Fecal pellets were collected once per week after BMT and intestinal microflora was characterized by RFLP analysis of 16S rRNA genes constructed from each sample of fecal pellets and digested with *HhaI*. Representative RFLP patterns are shown in mice with GVHD receiving diluent (a-e) and those with PMB (f-j) 7 days after BMT. Arrows indicate an OTU for *E coli*. (B) Time course changes in the proportion of *E coli* (n = 6-12 / group). Survival (C) and clinical GVHD scores (D, mean ± SE) after BMT are shown (n = 6-12/group). Data from 2 independent experiments were combined. (E) Numbers of donor (CD45.1$^+$) T cells in mLNs on day 5 (n = 20/group). (F) Pathology scores of the small intestine on day 7 (n = 20/group). Data from 3 independent experiments were combined and are shown as mean ± SE (*$P < .05$).

is one of the most frequent causes of death in patients with severe intestinal GVHD.

There are other interfaces that exist between the environment and the host, such as the skin and airways. Epithelial cells in these tissues can also release antimicrobial peptides such as β-defensins in response to bacteria and LPS.[47] GVHD-mediated epithelial cell damage of these tissues may also impair the local secretion of antimicrobial peptides, leading to aberrant overgrowth of pathogens and development of dermal infections or pneumonia, which are frequently observed in patients with GVHD. Furthermore, the development of these pathologic conditions may be associated with the unique tissue specificity of GVHD for tissues that are in contact with high microbial loads, such as the skin, liver, intestine, and lung.

Intestinal epithelial cells are continuously regenerated from ISCs, which are required to regenerate damaged sections of the intestinal epithelium.[48] Paneth cells are derived from ISCs and serve as a niche for ISCs.[8] Our previous[7] and current studies addressed intestinal GVHD at the cellular level, and demonstrated that ISCs and their niche Paneth cells could survive pretransplant conditioning and regenerate injured epithelium by conditioning in the absence of GVHD. However, both ISCs and Paneth cells are targeted by GVHD, resulting in an impairment of the physiologic repair mechanisms of injured epithelium, although it remains to be elucidated whether Paneth cell loss is induced by direct cytotoxicity to Paneth cell itself or secondary to the loss of ISCs. This phenomenon may explain the prolonged and refractory nature of clinical intestinal GVHD. These new insights will help to establish new therapeutic strategies that can be used to prevent and treat GVHD and related infections and improve the clinical outcome of allogeneic BMT.

Acknowledgments

This study was supported by grants from Japan Society for the Promotion of Science (JSJP) KAKENHI (23659490 to T.T., 23390193 to T.A., and 22592029 to K.N.), Health and Labor Science Research Grants (T.T.), the Foundation for Promotion of Cancer Research (Tokyo, Japan; to T.T.), the Knowledge Cluster, Sapporo Bio-S from Ministry of

Education, Culture, Sports, Science and Technology (MEXT; Tokyo, Japan; to T.A.), Yakult Bio-Science Foundation (Tokyo, Japan; to Y.E.), and SENSHIN Medical Research Foundation (to T.T.).

Authorship

Contribution: Y.E. and T.T. developed the conceptual framework of the study, designed the experiments, conducted studies, analyzed data, and wrote the paper; S.T., H.O., S. Shimoji, K.N., H.U., S. Shimoda, and H.I. conducted experiments; and N.S., T.A., and K.A. supervised experiments.

Conflict-of-interest disclosure: The authors declare no competing financial interests.

Correspondence: Takanori Teshima, Center for Cellular and Molecular Medicine, Kyushu University Hospital, 3-1-1 Maidashi, Higashi-ku, Fukuoka 812-8582, Japan; e-mail: tteshima@cancer.med.kyushu-u.ac.jp.

References

1. Bossaer JB, Hall PD, Garrett-Mayer E. Incidence of vancomycin-resistant enterococci (VRE) infection in high-risk febrile neutropenic patients colonized with VRE. *Support Care Cancer.* 2010; 19(2):231-237.
2. Winston DJ, Gale RP, Meyer DV, Young LS. Infectious complications of human bone marrow transplantation. *Medicine.* 1979;58(1):1-31.
3. van Bekkum D, Vos O. Treatment of secondary disease in radiation chimaeras. *Int J Radiat Biol.* 1961;3:173-181.
4. Jones JM, Wilson R, Bealmear PM. Mortality and gross pathology of secondary disease in germ-free mouse radiation chimeras. *Radiation Res.* 1971;45(3):577-588.
5. van Bekkum DW, Roodenburg J, Heidt PJ, van der Waaij D. Mitigation of secondary disease of allogeneic mouse radiation chimeras by modification of the intestinal microflora. *J Nat Cancer Inst.* 1974;52(2):401-404.
6. Heit H, Heit W, Kohne E, Fliedner TM, Hughes P. Allogeneic bone marrow transplantation in conventional mice: I. Effect of antibiotic therapy on long term survival of allogeneic chimeras. *Blut.* 1977;35(2):143-153.
7. Takashima S, Kadowaki M, Aoyama K, et al. The Wnt agonist R-spondin1 regulates systemic graft-versus-host disease by protecting intestinal stem cells. *J Exp Med.* 2011;208(2):285-294.
8. Sato T, van Es JH, Snippert HJ, et al. Paneth cells constitute the niche for Lgr5 stem cells in intestinal crypts. *Nature.* 2011;469(7330):415-418.
9. Selsted ME, Harwig SS. Determination of the disulfide array in the human defensin HNP-2. A covalently cyclized peptide. *J Biol Chem.* 1989; 264(7):4003-4007.
10. Ganz T, Selsted ME, Lehrer RI. Defensins. *Eur J Haematol.* 1990;44(1):1-8.
11. Salzman NH, Hung K, Haribhai D, et al. Enteric defensins are essential regulators of intestinal microbial ecology. *Nat Immunol.* 2010;11(1):76-83.
12. Eckburg PB, Bik EM, Bernstein CN, et al. Diversity of the human intestinal microbial flora. *Science.* 2005;308(5728):1635-1638.
13. Qin J, Li R, Raes J, et al. A human gut microbial gene catalogue established by metagenomic sequencing. *Nature.* 2010;464(7285):59-65.
14. Hill DA, Artis D. Intestinal bacteria and the regulation of immune cell homeostasis. *Ann Rev Immunol.* 2010;28:623-667.
15. Zoetendal EG, Akkermans AD, De Vos WM. Temperature gradient gel electrophoresis analysis of 16S rRNA from human fecal samples reveals stable and host-specific communities of active bacteria. *Appl Environ Microbiol.* 1998;64(10): 3854-3859.
16. Kurokawa K, Itoh T, Kuwahara T, et al. Comparative metagenomics revealed commonly enriched gene sets in human gut microbiomes. *DNA Res.* 2007;14(4):169-181.
17. Hooper LV, Macpherson AJ. Immune adaptations that maintain homeostasis with the intestinal microbiota. *Nature Rev Immunol.* 2010;10(3):159-169.
18. Heimesaat MM, Nogai A, Bereswill S, et al. MyD88/TLR9 mediated immunopathology and gut microbiota dynamics in a novel murine model of intestinal graft-versus-host disease. *Gut.* 2010; 59(8):1079-1087.
19. Ubeda C, Taur Y, Jenq RR, et al. Vancomycin-resistant Enterococcus domination of intestinal microbiota is enabled by antibiotic treatment in mice and precedes bloodstream invasion in humans. *J Clin Invest.* 2010;120(12):4332-4341.
20. Cooke KR, Kobzik L, Martin TR, et al. An experimental model of idiopathic pneumonia syndrome after bone marrow transplantation. I. The roles of minor H antigens and endotoxin. *Blood.* 1996;88: 3230-3239.
21. Asakura S, Hashimoto D, Takashima S, et al. Alloantigen expression on non-hematopoietic cells reduces graft-versus-leukemia effects in mice. *J Clin Invest.* 2010;120(7):2370-2378.
22. Teshima T, Ordemann R, Reddy P, et al. Acute graft-versus-host disease does not require alloantigen expression on host epithelium. *Nat Med.* 2002;8(6):575-581.
23. Ayabe T, Satchell DP, Wilson CL, Parks WC, Selsted ME, Ouellette AJ. Secretion of microbicidal alpha-defensins by intestinal Paneth cells in response to bacteria. *Nat Immunol.* 2000;1(2): 113-118.
24. Li F, Hullar MA, Lampe JW. Optimization of terminal restriction fragment polymorphism (TRFLP) analysis of human gut microbiota. *J Microbiol Methods.* 2007;68(2):303-311.
25. Hayashi H, Takahashi R, Nishi T, Sakamoto M, Benno Y. Molecular analysis of jejunal, ileal, caecal and recto-sigmoidal human colonic microbiota using 16S rRNA gene libraries and terminal restriction fragment length polymorphism. *J Med Microbiol.* 2005;54(Pt 11):1093-1101.
26. Simpson EH. Measurement of diversity. *Nature.* 1949;163:688.
27. Shannon C. A mathematical theory of communication. *Bell System Technol J.* 1948;27:379-423.
28. Ouellette AJ, Hsieh MM, Nosek MT, et al. Mouse Paneth cell defensins: primary structures and antibacterial activities of numerous cryptdin isoforms. *Infect Immun.* 1994;62(11):5040-5047.
29. Masuda K, Sakai N, Nakamura K, Yoshioka S, Ayabe T. Bactericidal activity of mouse alpha-defensin cryptdin-4 predominantly affects noncommensal bacteria. *J Innate Immun.* 2011;3(3): 315-326.
30. Liu WT, Marsh TL, Cheng H, Forney LJ. Characterization of microbial diversity by determining terminal restriction fragment length polymorphisms of genes encoding 16S rRNA. *Appl Environ Microbiol.* 1997;63(11):4516-4522.
31. Hayashi H, Sakamoto M, Benno Y. Phylogenetic analysis of the human gut microbiota using 16S rDNA clone libraries and strictly anaerobic culture-based methods. *Microbiol Immunol.* 2002; 46(8):535-548.
32. Ivanov II, Atarashi K, Manel N, et al. Induction of intestinal Th17 cells by segmented filamentous bacteria. *Cell.* 2009;139(3):485-498.
33. Shlomchik WD, Couzens MS, Tang CB, et al. Prevention of graft versus host disease by inactivation of host antigen-presenting cells. *Science.* 1999;285(5426):412-415.
34. Vaishnava S, Behrendt CL, Ismail AS, Eckmann L, Hooper LV. Paneth cells directly sense gut commensals and maintain homeostasis at the intestinal host-microbial interface. *Proc Natl Acad Sci U S A.* 2008; 105(52):20858-20863.
35. Mastroianni JR, Ouellette AJ. Alpha-defensins in enteric innate immunity: functional Paneth cell alpha-defensins in mouse colonic lumen. *J Biol Chem.* 2009;284(41):27848-27856.
36. Hooper LV, Midtvedt T, Gordon JI. How host-microbial interactions shape the nutrient environment of the mammalian intestine. *Annu Rev Nutr.* 2002;22:283-307.
37. Bäckhed F, Ley RE, Sonnenburg JL, Peterson DA, Gordon JI. Host-bacterial mutualism in the human intestine. *Science.* 2005;307(5717):1915-1920.
38. Ley RE, Turnbaugh PJ, Klein S, Gordon JI. Microbial ecology: human gut microbes associated with obesity. *Nature.* 2006;444(7122):1022-1023.
39. Turnbaugh PJ, Ley RE, Mahowald MA, Magrini V, Mardis ER, Gordon JI. An obesity-associated gut microbiome with increased capacity for energy harvest. *Nature.* 2006;444(7122):1027-1031.
40. Manichanh C, Rigottier-Gois L, Bonnaud E, et al. Reduced diversity of faecal microbiota in Crohn's disease revealed by a metagenomic approach. *Gut.* 2006;55(2):205-211.
41. Bollyky PL, Bice JB, Sweet IR, et al. The toll-like receptor signaling molecule Myd88 contributes to pancreatic beta-cell homeostasis in response to injury. *PLoS One.* 2009;4(4):e5063.
42. Penders J, Thijs C, van den Brandt PA, et al. Gut microbiota composition and development of atopic manifestations in infancy: the KOALA Birth Cohort Study. *Gut.* 2007;56(5):661-667.
43. Hill GR, Ferrara JL. The primacy of the gastrointestinal tract as a target organ of acute graft-versus-host disease: rationale for the use of cytokine shields in allogeneic bone marrow transplantation. *Blood.* 2000;95(9):2754-2759.
44. Nestel FP, Price KS, Seemayer TA, Lapp WS. Macrophage priming and lipopolysaccharide-triggered release of tumor necrosis factor alpha during graft-versus-host disease. *J Exp Med.* 1992;175:405-413.
45. Cooke KR, Gerbitz A, Crawford JM, et al. LPS antagonism reduces graft-versus-host disease and preserves graft-versus-leukemia activity after experimental bone marrow transplantation. *J Clin Invest.* 2001;107(12):1581-1589.
46. Gerbitz A, Schultz M, Wilke A, et al. Probiotic effects on experimental graft-versus-host disease: let them eat yogurt. *Blood.* 2004;103(11):4365-4367.
47. Bals R, Wang X, Meegalla RL, et al. Mouse beta-defensin 3 is an inducible antimicrobial peptide expressed in the epithelia of multiple organs. *Infect Immun.* 1999;67(7):3542-3547.
48. Sato T, Vries RG, Snippert HJ, et al. Single Lgr5 stem cells build crypt-villus structures in vitro without a mesenchymal niche. *Nature.* 2009; 459(7244):262-265.

blood

2012 119: 2263-2273
Prepublished online January 18, 2012;
doi:10.1182/blood-2011-04-351965

CIN85 is required for Cbl-mediated regulation of antigen receptor signaling in human B cells

Hiroaki Niiro, Siamak Jabbarzadeh-Tabrizi, Yoshikane Kikushige, Takahiro Shima, Kumiko Noda, Shun-ichiro Ota, Hirofumi Tsuzuki, Yasushi Inoue, Yojiro Arinobu, Hiromi Iwasaki, Shinji Shimoda, Eishi Baba, Hiroshi Tsukamoto, Takahiko Horiuchi, Tadayoshi Taniyama and Koichi Akashi

Blood (print ISSN 0006-4971, online ISSN 1528-0020), is published weekly by the American Society of Hematology, 2021 L St, NW, Suite 900, Washington DC 20036.

CIN85 is required for Cbl-mediated regulation of antigen receptor signaling in human B cells

Hiroaki Niiro,[1] Siamak Jabbarzadeh-Tabrizi,[1] Yoshikane Kikushige,[2] Takahiro Shima,[1] Kumiko Noda,[1] Shun-ichiro Ota,[1] Hirofumi Tsuzuki,[1] Yasushi Inoue,[1] Yojiro Arinobu,[2] Hiromi Iwasaki,[2] Shinji Shimoda,[1] Eishi Baba,[1] Hiroshi Tsukamoto,[1] Takahiko Horiuchi,[1] Tadayoshi Taniyama,[3] and Koichi Akashi[1]

[1]Department of Medicine and Biosystemic Science, Graduate School of Medical Sciences, Kyushu University, Fukuoka, Japan; [2]Center for Cellular and Molecular Medicine, Kyushu University Hospital, Fukuoka, Japan; and [3]Laboratory of Bacterial Infection and Immunity, Department of Immunology, National Institute of Infectious Diseases, Tokyo, Japan

The aberrant regulation of B-cell receptor (BCR) signaling allows unwanted B cells to persist, thereby potentially leading to autoimmunity and B-cell malignancies. Casitas B-lineage lymphoma (Cbl) proteins suppress BCR signaling; however, the molecular mechanisms that control Cbl function in human B cells remain unclear. Here, we demonstrate that CIN85 (c-Cbl interacting protein of 85 kDa) is constitutively associated with c-Cbl, Cbl-b, and B-cell linker in B cells. Experiments using CIN85-overexpressing and CIN85-knockdown B-cell lines revealed that CIN85 increased c-Cbl phosphorylation and inhibited BCR-induced calcium flux and phosphorylation of Syk and PLCγ2, whereas it did not affect BCR internalization. The Syk phosphorylation in CIN85-overexpressing and CIN85-knockdown cells was inversely correlated with the ubiquitination and degradation of Syk. Moreover, CIN85 knockdown in primary B cells enhanced BCR-induced survival and growth, and increased the expression of BcLxL, A1, cyclin D2, and myc. Following the stimulation of BCR and Toll-like receptor 9, B-cell differentiation-associated molecules were up-regulated in CIN85-knockdown cells. Together, these results suggest that CIN85 is required for Cbl-mediated regulation of BCR signaling and for downstream events such as survival, growth, and differentiation of human B cells. (*Blood.* 2012;119(10):2263-2273)

Introduction

B-cell receptor (BCR) signaling guides critical cell fate decisions in B cells during ontogeny.[1,2] BCRs can generate tolerogenic signals to purge or silence B cells that bind to self-antigens, and immunogenic signals to expand B cells that are specific for foreign antigens. Thus, BCR signaling must be properly regulated at the various stages of B-cell development, as aberrant regulation of BCR signaling potentially leads to autoimmunity and B-cell malignancies.

On BCR ligation by antigens, the Src-family protein tyrosine kinase (PTK) Lyn and Syk are initially activated. Syk propagates the signal by phosphorylating downstream signaling molecules, causing the activation of critical signaling intermediates phosphoinositol 3-kinase (PI3K) and phospholipase C (PLC)γ2. PI3K activates Akt kinase, which is important for B-cell survival.[3] PLCγ2 activation induces the release of intracellular Ca^{2+} and the activation of protein kinase C (PKC), which cause the activation of mitogen-activated protein kinases (MAPKs; ERK, JNK, and p38 MAPK) and of transcription factors, including NF-κB and NF-AT. These molecules regulate further downstream molecules that are responsible for determining B-cell fates such as survival, growth, and differentiation.[1,2]

Casitas B-lineage lymphoma (Cbl) proteins are E3 ubiquitin ligases that regulate signals of various receptors by promoting the ubiquitination of signaling components.[4,5] Tyrosine phosphorylation of Cbl proteins is critical for their function.[6] Mammalian Cbl proteins consist of 3 members, c-Cbl, Cbl-b, and Cbl-3, among which c-Cbl and Cbl-b are expressed in hematopoietic cells.[7] In B cells, Cbl proteins associate with Syk and B-cell linker (BLNK), and negatively regulate BCR signaling.[8,9] B cell-specific ablation of c-Cbl/Cbl-b proteins in mice causes aberrant BCR signaling as well as impaired B-cell anergy, culminating in the development of systemic lupus erythematosus (SLE)–like disease.[10] In addition, c-Cbl is hypophosphorylated on tyrosine in advanced stages of chronic lymphocytic leukemia (CLL).[11] These findings suggest that Cbl-mediated regulation of BCR signaling is critical for the fate decisions of self-reactive and malignant B cells.

Adaptors are noncatalytic molecules that integrate the spatial and temporal assembly of multiprotein complexes involved in the survival, growth, and differentiation of B cells. We previously showed that the B lymphocyte adaptor molecule of 32 kDa (Bam32)/DAPP1 regulates BCR signaling/internalization and B-cell survival.[12,13] The *SH3KBP1* (SH3-domain kinase-binding protein 1) gene, which is also known as CIN85 (c-Cbl interacting protein of 85 kDa), encodes an adaptor that is independently identified by several groups and contains 3 SH3 domains, a proline-rich region, and a coiled-coil domain.[14-17] Early studies showed that in nonimmune cells, CIN85 regulates the clathrin-dependent internalization of receptor tyrosine kinases (RTKs) such as epidermal growth factor receptors (EGFRs).[18,19] The formation of the ternary complex of CIN85, c-Cbl, and endophillin is critical for this process. In immune cells, however, little is known approximately the function of CIN85. CIN85 facilitates ligand-induced FcεRI internalization in RBL-2H3 mast cells.[20] In addition, it regulates FcεRI signaling via Cbl-mediated regulation of

Submitted April 29, 2011; accepted January 13, 2012. Prepublished online as *Blood* First Edition paper, January 18, 2012; DOI 10.1182/blood-2011-04-351965.

The online version of this article contains a data supplement.

The publication costs of this article were defrayed in part by page charge payment. Therefore, and solely to indicate this fact, this article is hereby marked "advertisement" in accordance with 18 USC section 1734.

Syk expression in RBL-2H3 cells.[21] A recent study showed that CIN85 modulates c-Cbl–mediated down-regulation of FcγRIIa in human neutrophils.[22] It is thus of interest to determine whether CIN85 regulates the signaling pathways of other multimeric immune receptors, such as the T- and B-cell receptors.

Here, we demonstrate that CIN85 is constitutively associated with c-Cbl, Cbl-b, and BLNK in human B cells. Gain-of-function and loss-of-function experiments revealed that CIN85 up-regulated c-Cbl phosphorylation and inhibited BCR-induced calcium flux and phosphorylation of Syk and PLCγ2, without affecting BCR internalization. CIN85 also promoted c-Cbl–dependent ubiquitination and degradation of Syk. Moreover, CIN85 knockdown in primary B cells caused enhanced BCR-induced survival and growth, and augmented BCR/TLR9-induced expression of B-cell differentiation-associated molecules. Collectively, these results suggest that CIN85 is required for Cbl-mediated regulation of BCR signaling and for downstream events such as the survival, growth, and differentiation of human B cells.

Methods

Reagents

Goat anti–human IgM and IgG/IgA/IgM F(ab′)$_2$ fragments were purchased from Jackson ImmunoResearch Laboratories. Rabbit anti–human phospho-Zap-70 (Y319)/Syk (Y352), anti–human phospho-PLCγ2 (Y1217), anti–human phospho-Akt, anti–mouse Akt, anti–human phospho-JNK, anti–human phospho-ERK, and anti–human PLCγ2 pAbs as well as anti–human BclxL and Blimp-1 mAbs were purchased from Cell Signaling Technology. Mouse anti–human phospho-Btk, anti–human phospho-BLNK, anti–human c-Cbl, and anti–human Rac1 mAbs were from BD Immunocytometry. Mouse anti–human Cbl-b, anti–human Syk (4D10), anti–human BLNK, and anti-ubiquitin mAbs as well as rabbit anti–human c-Cbl and anti–mouse cyclin D2 pAbs were from Santa Cruz Biotechnology. Mouse anti-V5 mAb was from Invitrogen. Mouse anti-phosphotyrosine and anti–human CIN85 mAbs were from Upstate Biotechnology. Rabbit anti–human Vav2 mAb was from Epitomics. Sheep anti–human CD2AP pAb was from R&D Systems. Mouse anti–β-actin mAb was from Sigma-Aldrich.

B cell lines and primary B cells

The B lymphoma cell line BJAB was cultured in RPMI 1640 medium supplemented with 10% FCS. Human peripheral blood mononuclear cells, kindly provided by healthy volunteers, were separated from their buffy coats. Informed consent was obtained from all subjects in accordance with the Declaration of Helsinki. The Institutional Review Board of Kyushu University Hospital approved all research on human subjects. B cells were isolated with Dynabeads M450 CD19 and DETACHaBEAD CD19 (Dynal Biotech), according to the manufacturer's instructions. The isolated B cells exhibited greater than 99.5% viability on trypan blue exclusion and more than 95% purity on flow cytometry. Trace levels of phosphorylation of BCR-signaling molecules were observed in the B cells immediately after purification, probably because of mechanical stress.[23] The cells were thus rested for a couple of hours before further analysis. The cells were cultured at a density of 1×10^6 cells/mL in a 96 flat-bottom microtiter plate in complete RPMI 1640 medium supplemented with 10% FCS.

Expression constructs and transfection

Constructs encoding V5-tagged wild-type (WT) and 3 SH3 domain-deleted mutants of human CIN85 (pEF1/V5-CIN85 and –CIN85-dSH3ABC) were previously described.[24] The BJAB cells were transfected with the aforementioned constructs using a Gene Pulser apparatus (Bio-Rad Laboratories). The control cells were transfected with an empty vector. Stably transfected BJAB clones were selected in the presence of G418 (2 mg/mL) and screened with anti-V5 mAb.

RNA interference

The pSUPER-based strategy was adopted to knockdown hCIN85 expression. To generate CIN85 small-hairpin RNA (shRNA), a 19-nucleotide sequence (CAGCAATGACATTGACTTA) selected from human CIN85 cDNA was annealed and ligated into the pSUPER or GFP-pSUPER vector. A scrambled sequence (GTTACTAACGCGAATTAAC) was used as negative control. hCIN85 or the control shRNA vector was transfected into BJAB cells using a Gene Pulser apparatus, and stable hCIN85-knockdown BJAB clones were selected in the presence of puromycin (0.5 μg/mL). Transient transfections of primary B cells with the pSUPER-hCIN85 vector were performed using the Nucleofection kit from AMAXA Biosystems as previously described.[23]

Measurement of intracellular free calcium

B cells were washed with RPMI 1640 medium containing 10% FCS and adjusted to a concentration of 1×10^6 cells/mL. After incubation at 37°C for 15 minutes, 1 μg/mL of Fluo 4/AM (Dojindo) was added, and the cells were incubated for an additional 30 to 45 minutes with resuspension every 15 minutes. The cells were centrifuged and resuspended in RPMI 1640 at a density of 2×10^6 cells/mL and stimulated with anti-IgM (20 μg/mL). The fluorescence intensity of intracellular Fluo 4 was monitored and analyzed using flow cytometry.

Immunoprecipitation

Cells were lysed as described.[13] Subsequently, protein G-Sepharose (Amersham Pharmacia Biotech) precleared lysates were incubated with anti-V5, -BLNK, -Syk, -Cbl, -Vav2 mAb, or -CD2AP pAb for 1 hour at 4°C and then immunoprecipitated with protein G-Sepharose overnight at 4°C. The precipitated proteins were resolved by 10% SDS-PAGE; transferred onto a Millipore Immobilon polyvinylidene difluoride membrane; and blotted with anti-phosphotyrosine (4G10), -V5, -c-Cbl, -Cbl-b, -BLNK, -Vav2, -Syk, or -ubiquitin mAbs, followed by incubation with secondary HRP-conjugated IgG (Jackson ImmunoResearch Laboratories) specific for the primary Ab. The blots were developed with an ECL Plus kit (Amersham Biosciences).

Western blot analysis

Nonstimulated or stimulated cells (1×10^6) were lysed as described.[12] The lysates were then denatured in an equal volume of 2 × SDS sample buffer, resolved on a 10% SDS-PAGE gel, and electro-transferred to nitrocellulose membranes in non-SDS–containing transfer buffer (25mM Tris, 0.2M glycine, and 20% methanol; pH 8.5). Western blotting was performed with anti–phospho-Syk (1:2000), anti–phospho-PLCγ2 (1:2000), anti–phospho-BLNK (1:2000), anti–phospho-JNK (1:2000), anti–phospho-ERK (1:2000), anti–phospho-Akt (1:2000), anti-Akt (1:2000), anti-CIN85 (1:2000), anti–β-actin (1:2000), or anti-Vav2 (1:2000), followed by a 1:15 000 dilution of anti–rabbit or anti–mouse HRP-conjugated IgG. The blots were developed with the ECL plus kit (Amersham Biosciences). The chemiluminescence intensity was monitored using a Laser3000 (FujiFilm) instrument. We quantitated the band intensity of the proteins using ImageGauge Version 4.22 software (FujiFilm). The resulting values were expressed as fold changes in protein expression relative to the protein expression in unstimulated control cells.

Luciferase assays

Cells (1×10^7) were transfected by electroporation with the NF-AT-reporter construct, which was generously provided by Dr Shoichiro Miyatake (The Tokyo Metropolitan Institute of Medical Science, Tokyo, Japan). After 18 to 20 hours, cells were harvested and plated on 96-well plates at a density of 2×10^5/well. Triplicate cultures were incubated in the media alone with graded doses of anti-IgM or with 50nM PMA and 2.5μM ionomycin. After 6 hours, the cells were lysed in 50 μL reporter lysis buffer (Promega) for 15 minutes at room temperature. The luciferase activity was assayed by adding 20 μL luciferase substrate (Promega) to 50 μL lysate

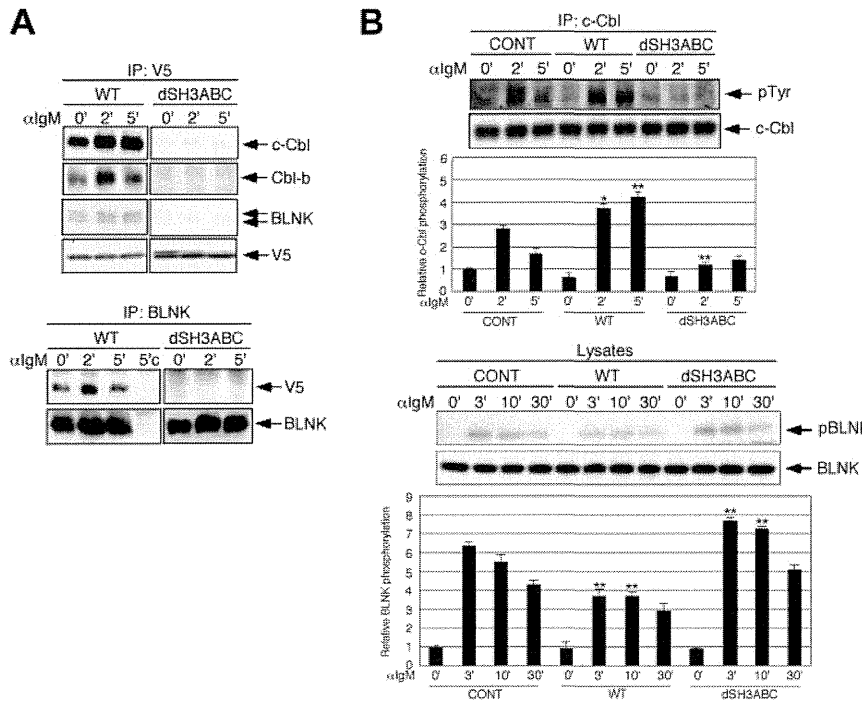

Figure 1. CIN85 associates with Cbl and BLNK and regulates their phosphorylation in B cells. (A) BJAB cells stably expressing either WT or SH3-deleted CIN85 were stimulated with 20 μg/mL of F(ab′) $_2$ goat anti–human IgM for the indicated time periods. Immunoprecipitates with anti-V5 or anti-BLNK mAb were separated on a 10% SDS-PAGE gel and analyzed by Western blotting with anti–c-Cbl, anti–Cbl-b, anti-BLNK, or anti-V5 mAb. 5′c, immunoprecipitation of the cell lysates at 5 minutes with isotype control. (B) Control BJAB cells and stable transformants expressing either WT or SH3-deleted CIN85 were stimulated with 20 μg/mL of F(ab′) $_2$ goat anti–human IgM for the indicated time periods. Immunoprecipitates with anti–c-Cbl mAb were separated on a 10% SDS-PAGE gel and analyzed by Western blotting with anti-phosphotyrosine or anti–c-Cbl mAb. The resulting values are expressed as fold changes in protein expression compared with unstimulated control cells. The values are the mean ± SD of 3 independent experiments (*$P < .05$, **$P < .01$ *vs controls*). (C) Control BJAB cells and stable transformants expressing either WT or SH3-deleted CIN85 were stimulated with 20 μg/mL of F(ab′) $_2$ goat anti–human IgM for the indicated time periods. The cell lysates were subsequently separated on a 10% SDS-PAGE gel and analyzed by Western blotting with anti–phospho-BLNK or anti-BLNK mAb. The resulting values are expressed as fold changes in protein expression compared with unstimulated control cells. The values are the mean ± SD of 3 independent experiments (**$P < .01$ vs controls).

and immediately measuring the luminescence on a Lumat LB9507 luminometer (EG & G Berthold). To serve as a control for the transfection efficiency, the relative luciferase activity of the medium and cells stimulated with BCR was calculated relative to stimulation with PMA/ionomycin.

Flow cytometric analysis

BJAB cells were incubated on ice for 15 minutes with 20 μg/mL goat-unlabeled anti-IgM before they were washed with ice-cold medium and warmed at 37°C for the indicated time intervals. The cells were washed with ice-cold PBS containing 2% FBS and 0.2% sodium azide (Fisher Scientific) to stop internalization at the assigned time points and to remove the unbound Ab. The remaining surface BCRs were stained with FITC-labeled rabbit anti–goat Ig and quantified by flow cytometry. The data are presented as the percentage of surface BCR remaining.

Fluorescence microscopic analysis

BJAB cells were incubated with 10 μg/mL of unlabeled goat anti–human IgM sera (20 μg/mL) at 4°C for 30 minutes and warmed to 37°C for the indicated time periods. The cells were then fixed with 3.7% paraformaldehyde and permeabilized with PBS containing 1% BSA and 0.05% saponin (wash buffer). The cells were then incubated for 30 minutes with FITC-conjugated anti–goat IgG pAb (Jackson ImmunoResearch Laboratories) at 4°C. The stained cells were centrifuged onto slides and analyzed with inverted fluorescent microscopy (BZ-9000; Keyence).

Quantitative real-time PCR

The total RNA was extracted from the primary B cells using Isogen reagent (Nippon gene) and was treated with DNase I (Invitrogen) to remove contaminating genomic DNA. First-strand cDNA was synthesized using a QuantiTect reverse transcription kit (QIAGEN). Quantitative real-time PCR was performed in the ABI Prism 7700 Sequence Detector (Applied Biosystems). The reactions were performed in triplicate wells in 96-well plates. TaqMan target mixes for Cyclin D2, Myc, *BCL2L1*/BclxL, *BCL2A1*/A1, *PRDM1*/Blimp-1, and *XBP1* were purchased from Applied Biosystems. 18S ribosomal RNA (rRNA) was separately amplified in the same plate as an internal control for variation in the amount of cDNA in PCR. The collected data were analyzed using the Sequence Detector software (Applied Biosystems). The data were expressed as the fold change in gene expression relative to the expression in the control cells.

Annexin V staining

After culture, cells (1-2 × 10^5) were washed twice with PBS and suspended in 85 μL binding buffer (MBL) containing Ca^{2+}. The cell suspension supplemented with 10 μL annexin-V–FITC or annexin-V–PE (MBL) and 5 μg of propidium iodide (PI) or 1 μg of 7-ADD was incubated at room temperature for 15 minutes in the dark. Subsequently, binding buffer was added, and the fraction of early apoptotic cells was measured using flow cytometry.

BrdU assay

DNA synthesis was monitored by pulse-labeling cells for 2 hours with the thymidine analog 5-bromo-2′-deoxyuridine (BrdU). The cells were washed 3 times with PBS and fixed for 20 minutes at −20°C in an ethanol fixative (0.15mM glycine in 70% EtOH, pH 2.0). After rehydration in PBS, BrdU incorporation was detected by incubation with an anti-BrdU mAb for 1 hour at 37°C, followed by a rhodamine-conjugated anti–mouse antibody (1:500; Jackson ImmunoResearch Laboratories) and staining of the nucleus with 4′-6-diamidino-2-phenylindole for 1 hour. The proportion of BrdU-positive nuclei (BrdU labeling index) was assessed, based on a sample size of 500 cells per data point.

Statistical analysis

Statistical analysis was performed using the Student *t* test. $P < .05$ was considered statistically significant.

Results

CIN85 associates with Cbl and BLNK and regulates their phosphorylation

The tyrosine phosphorylation of signaling molecules is a critical event in BCR signaling.[1,2] Because SH3 domains play an important role in the function of CIN85,[25] we focused on

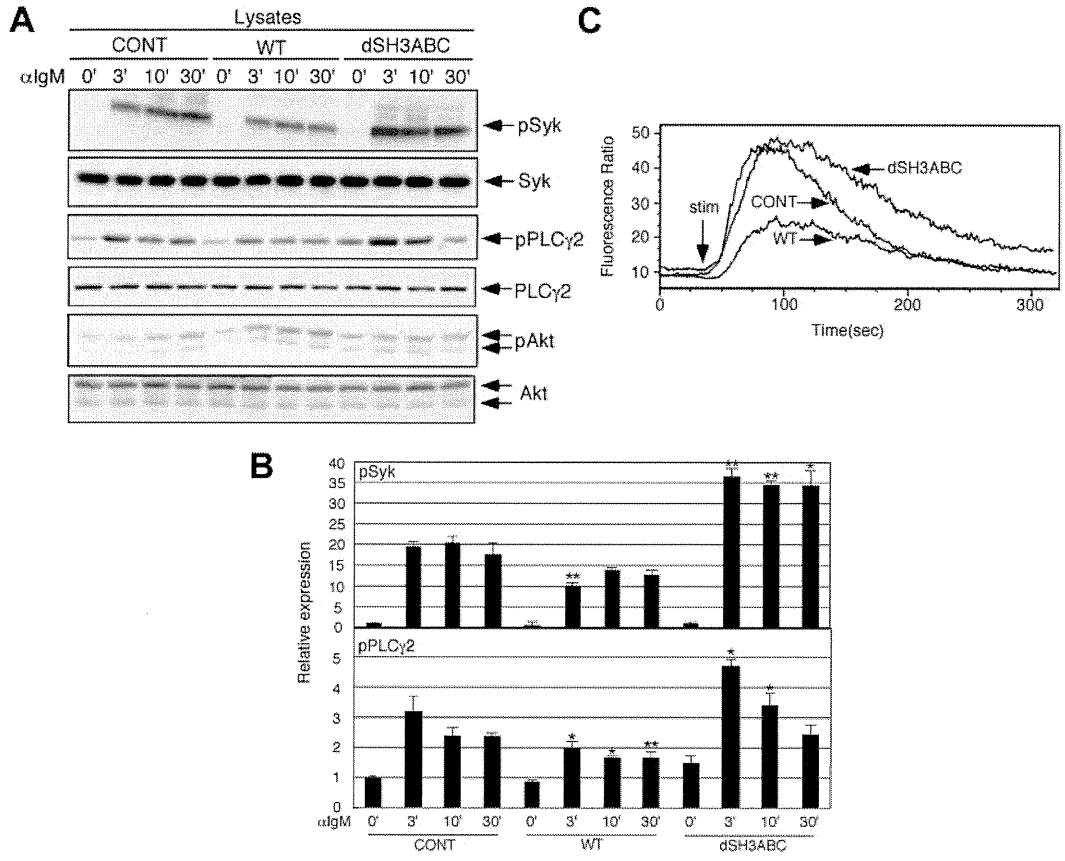

Figure 2. Forced CIN85 expression inhibits BCR-induced calcium flux and phosphorylation of Syk and PLCγ2. (A-B) Control BJAB cells and stable transformants expressing either WT or SH3-deleted CIN85 were stimulated with 20 μg/mL of $F(ab')_2$ goat anti–human IgM for the indicated time periods. The cell lysates were subsequently separated on a 10% SDS-PAGE gel and analyzed by Western blotting with anti–phospho-Syk pAb, anti-Syk mAb, anti–phospho-PLCγ2 pAb, anti-PLCγ2 pAb, anti–phospho-Akt pAb, or anti-Akt pAb. The resulting values are expressed as fold changes in protein expression compared with unstimulated control cells. The values are the mean ± SD of 3 independent experiments (*$P < .05$, **$P < .01$ vs controls). (C) Ca^{2+} influx in control BJAB cells and stable transformants expressing either WT or SH3-deleted CIN85. The intracellular free calcium levels in Fluo 4/AM-loaded cells were analyzed using flow cytometry after the cells were stimulated with 20 μg/mL $F(ab')_2$ goat anti–human IgM. The results shown are representative of 4 independent experiments.

tyrosine-phosphorylated molecules downstream of the BCR that could associate with the SH3 domains of CIN85. Specifically, we focused on the 2 molecules, BLNK and c-Cbl, that function as key positive and negative regulators of BCR signaling,[1,10] respectively; both proteins can associate with the SH3 domains of CIN85.[14,26]

We first determined the association of Cbl and BLNK with CIN85 using WT and SH3-deleted CIN85-expressing B cell lines. Consistent with previous reports,[14,26] WT CIN85 was constitutively associated with c-Cbl and BLNK, and these associations were increased after BCR stimulation (Figure 1A). Cbl-b was similarly associated with WT CIN85, albeit to a lesser extent. Although the association of WT CIN85 and BLNK appeared modest, the inverse immunoprecipitation of BLNK confirmed the association (Figure 1A). As expected, the association of Cbl and BLNK with CIN85 was abrogated in SH3-deleted CIN85-expressing B cells, suggesting that the SH3 domains of CIN85 are required for its association with Cbl and BLNK. Because the tyrosine phosphorylation of c-Cbl and BLNK is critical for their function,[6,27] we next determined whether the overexpression of WT and SH3-deleted CIN85 affects BCR-induced phosphorylation of c-Cbl and BLNK. Compared with control cells, WT and SH3-deleted CIN85 sustained and inhibited c-Cbl phosphorylation, respectively (Figure 1B). In addition, WT and SH3-deleted CIN85 inhibited and enhanced BLNK phosphorylation, respectively (Figure 1B). These findings suggest that CIN85 associates with Cbl and BLNK and regulates their phosphorylation in an opposite manner.

Forced CIN85 expression inhibits BCR-induced calcium flux and the phosphorylation of Syk and PLCγ2

We tested whether the overexpression of WT and SH3-deleted CIN85 affects early BCR signaling. Syk phosphorylation, which is one of the earliest events in BCR signaling, was inhibited in WT CIN85-expressing cells, whereas it was sustained in SH3-deleted CIN85-expressing cells (Figure 2A-B). Two enzymes, PLCγ2 and PI3K, function as critical mediators downstream of BCR signaling.[1,2,28] WT and SH3-deleted CIN85 partially inhibited and enhanced BCR-induced phosphorylation of PLCγ2, respectively (Figure 2A-B). In contrast, the phosphorylation of Akt, which is a downstream molecule of PI3K, was not affected in WT or SH3-deleted CIN85-expressing cells (Figure 2A). Activated PLCγ2 converts PIP2 into IP3 and diacyl glycerol, of which PIP2 is critical for calcium flux in B cells.[1,2,12] Consistent with the levels of PLCγ2 phosphorylation, the BCR-induced calcium flux was significantly inhibited in WT CIN85-expressing cells, whereas it was slightly sustained in SH3-deleted CIN85-expressing cells (Figure 2C). These results suggest that CIN85 inhibits BCR-induced calcium flux and the

phosphorylation of Syk and PLCγ2, and that the SH3 domains of CIN85 are required for its inhibitory function.

CIN85 knockdown enhances BCR-induced calcium flux and the phosphorylation of Syk, Vav2, and PLCγ2, leading to augmented NF-AT activation and CD69 expression

To elucidate the role of endogenously expressed CIN85 in BCR signaling, we generated CIN85-knockdown B cell lines. In contrast to the CIN85-overexpressing cells (Figures 1 and 2), CIN85-knockdown cells exhibited enhanced phosphorylation of Syk, BLNK, and PLCγ2 (Figure 3A-B). Akt phosphorylation was comparable between control and CIN85-knockdown cells (Figure 3A). Consistent with the levels of PLCγ2 phosphorylation, BCR-induced calcium flux was accentuated in CIN85-knockdown cells (Figure 3C). Vav2 positively regulates PLCγ2 activation in B cells.[29] Vav2 phosphorylation was enhanced in CIN85-knockdown cells (Figure 3D). These BCR signaling profiles in CIN85-knockdown cells are reminiscent of those in c-Cbl/Cbl-b double-knockout B cells.[10] The phosphorylation of c-Cbl was significantly inhibited in CIN85-knockdown cells (Figure 3E). BCR-induced calcium flux plays a crucial role in the activation of the transcription factor NF-AT, the disruption of which results in significant defects in B-cell function.[30] BCR-induced NF-AT activation was enhanced in CIN85-knockdown cells (Figure 3F). In addition, BCR-induced up-regulation of the activation marker CD69 was pronounced in CIN85-knockdown cells (Figure 3G). These phenotypes in CIN85-knockdown cells were again similar to those observed in Cbl-deficient B cells.[10] Given that CIN85 strongly associates with Cbl proteins (Figure 1A), these results suggest that CIN85 plays a vital role in Cbl-mediated regulation of BCR signaling.

CIN85 promotes the ubiquitination and degradation of Syk in B cells

Cbl proteins function as E3 ubiquitin ligases and target PTK substrates, including Syk, for degradation.[31,32] We thus tested whether CIN85 affects Syk ubiquitination in B cells. Syk ubiquitination was induced on BCR stimulation. Compared with control cells, Syk ubiquitination was increased in WT CIN85-expressing cells (Figure 4A). In contrast, an impairment in Syk ubiquitination was noted in CIN85-knockdown cells (Figure 4A). These results suggest that CIN85 positively regulates Cbl-mediated ubiquitination of BCR-signaling molecules including Syk. Despite the altered levels of Syk ubiquitination, the level of total Syk protein was not altered in the WT CIN85-expressing or CIN85-knockdown cells throughout the stimulation (Figures 2A and 3A). Because only a small pool of Syk is phosphorylated on stimulation and targeted for degradation in B cells,[31] we tested the degree of Syk phosphorylation among the total Syk immunoprecipitate. The levels of phosphorylated Syk were reduced in WT CIN85-expressing cells but enhanced in CIN85-knockdown cells (Figure 4B), suggesting that CIN85 promotes Cbl-dependent loss of the phosphorylated pool of Syk in B cells.

CIN85 does not affect BCR internalization

CIN85 regulates Cbl-mediated internalization of the EGFR in several cell types other than B cells.[18,19] To test whether CIN85 affects BCR internalization, we first monitored the levels of surface BCR expression after stimulation. Without stimuli, the levels of surface BCR were similar on CIN85 overexpression and CIN85 knockdown. In parental cells, BCR crosslinking caused a rapid decrease in surface BCR levels, suggesting that BCR was efficiently internalized after stimulation (Figure 5A; supplemental Figure 1A, available on the *Blood* Web site; see the Supplemental Materials link at the top of the online article). BCR internalization was not affected in the WT or SH3-deleted CIN85-expressing cells. Moreover, the absence of endogenous CIN85 did not affect BCR internalization (Figure 5B, supplemental Figure 1A). Next, we directly visualized BCRs in B cell lines using fluorescence microscopy. In control cells, the BCR complexes exhibited a slightly patchy distribution before stimulation, and within 3 minutes after stimulation, the BCRs formed polarized tight caps on the cell surface. After 10 minutes of BCR stimulation, a punctate pattern of internalized BCRs was clearly visualized (Figure 5C). Consistent with the findings obtained with flow cytometry (Figure 5A-B), the spatial and temporal distribution of BCR complexes in CIN85-overexpressing and CIN85-knockdown cells appeared similar to that in control cells (Figure 5C, supplemental Figure 1B-C). These findings suggest that CIN85 does not affect BCR internalization.

CIN85 knockdown enhances the survival, growth, and differentiation of primary B cells

BCR signaling plays a critical role in determining the survival, growth, and differentiation of B cells.[1] It was thus of interest to test whether CIN85 affects B cell fate. A major obstacle, however, is that the survival, growth, and differentiation of B cell cannot be properly assessed in transformed B cells. We therefore sought to knock down CIN85 expression in human primary B cells. After introduction of the GFP-CIN85 knockdown vector, GFP-positive B cells were sorted and used for further experimentation. Under these conditions, we were able to knock down the CIN85 mRNA expression in B cells by 60%-80% (Figure 6A).

We first tested whether CIN85 knockdown affects the expression of the B-cell survival-associated genes BcLxL and A1. Consistent with previous studies,[33] BCR stimulation induced BcLxL and A1 mRNA expression in control cells. This induction was far more drastic in CIN85-knockdown B cells (Figure 6A). The costimulation of TLR9 with its ligand CpG enhances BCR-induced expression of B-cell survival genes.[34] This enhancement was less evident in CIN85-knockdown cells than in control cells (Figure 6A), suggesting that CIN85 knockdown requires less costimulation for the full induction of B-cell survival genes. Consistent the findings for the transcript levels, the BCR-induced expression of BcLxL protein was more pronounced in CIN85-knockdown cells (Figure 6B). We also tested whether CIN85 knockdown affects BCR-induced death of B cells using the annexin-binding assay. The CIN85-knockdown cells exhibited less BCR-induced cell death (Figure 6C). We next tested whether CIN85 knockdown affects the expression of the B-cell growth-associated genes cyclin D2 and myc. Again, BCR-induced expression of these genes was more pronounced in CIN85-knockdown cells (Figure 6A), and costimulation with TLR9 did not enhance induction compared with the control cells. Consistent with the findings for the transcript levels, BCR-induced expression of cyclin D2 protein was more pronounced in CIN85-knockdown cells (Figure 6B). We also tested whether CIN85 knockdown affects B-cell growth using the BrdU uptake assay. Consistent with the expression levels of cyclin D2 and myc, CIN85 knockdown enhanced BCR-induced cell growth (Figure 6D). On activation, B cells undergo plasma cell differentiation along with the expression of critical differentiation-associated genes such as Blimp-1 and Xbp-1. Consistent with previous studies,[35] BCR stimulation alone was not sufficient to induce the expression of Blimp-1 and Xbp-1 in human B cells (data not shown). However, the combined stimulation of BCR and TLR9 clearly induced the expression of these genes in control cells,

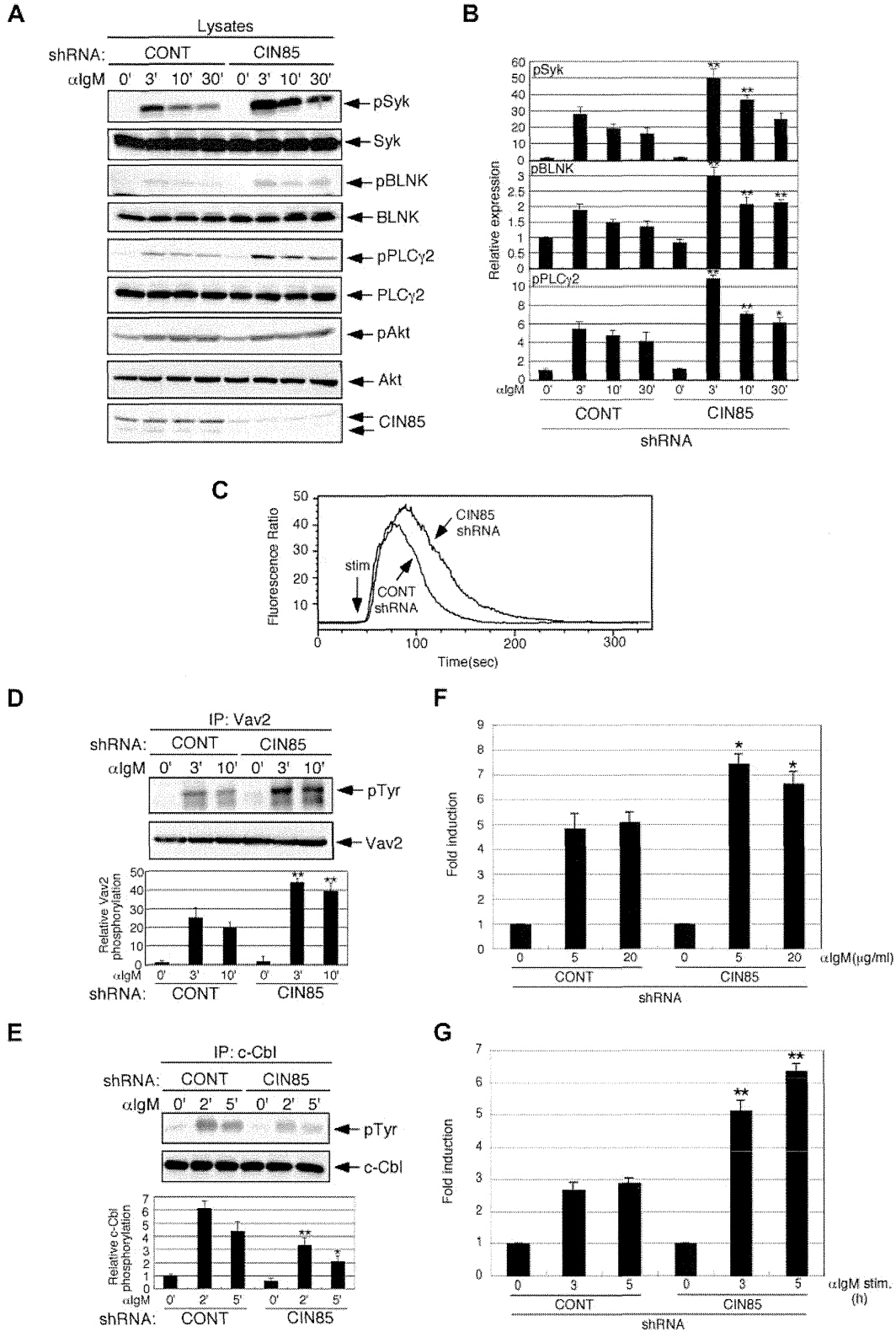

Figure 3. CIN85 knockdown enhances BCR-induced calcium flux and phosphorylation of Syk, Vav2, and PLCγ2, leading to augmented NF-AT activation and CD69 expression. (A-B) Stable control and CIN85-knockdown BJAB cells were stimulated with 20 μg/mL F(ab') $_2$ goat anti–human IgM for the indicated time periods. The cell lysates were subsequently separated on a 10% SDS-PAGE gel and analyzed by Western blotting with anti–phospho-Syk pAb, anti-Syk mAb, anti–phospho-BLNK mAb, anti-BLNK mAb, anti–phospho-PLCγ2 pAb, anti-PLCγ2 pAb, anti–phospho-Akt pAb, anti-Akt pAb, or anti-CIN85 mAb. The resulting values are expressed as fold changes in protein expression compared with unstimulated control cells. The values are the mean ± SD of 3 independent experiments (*$P < .05$, **$P < .01$ vs controls). (C) Ca^{2+} influx in stable control and CIN85-knockdown BJAB cells. Intracellular free calcium levels in Fluo 4/AM-loaded cells were analyzed using flow cytometry after the cells were stimulated with 20 μg/mL F(ab')$_2$ goat anti–human IgM. The results shown are representative of 4 independent experiments. (D-E) Stable control and CIN85-knockdown BJAB cells were stimulated with 20 μg/mL F(ab')$_2$ goat anti–human IgM for the indicated time periods. Immunoprecipitates with anti-Vav2 or anti–c-Cbl mAb were separated on a 10% SDS-PAGE gel and analyzed by Western blotting with anti-phosphotyrosine mAb, anti-Vav2 mAb, or anti–c-Cbl mAb. The resulting values are expressed as fold changes in protein expression compared with unstimulated control cells. The values are the mean ± SD of 3 independent experiments (*$P < .05$, **$P < .01$ vs controls). (F) Stable control

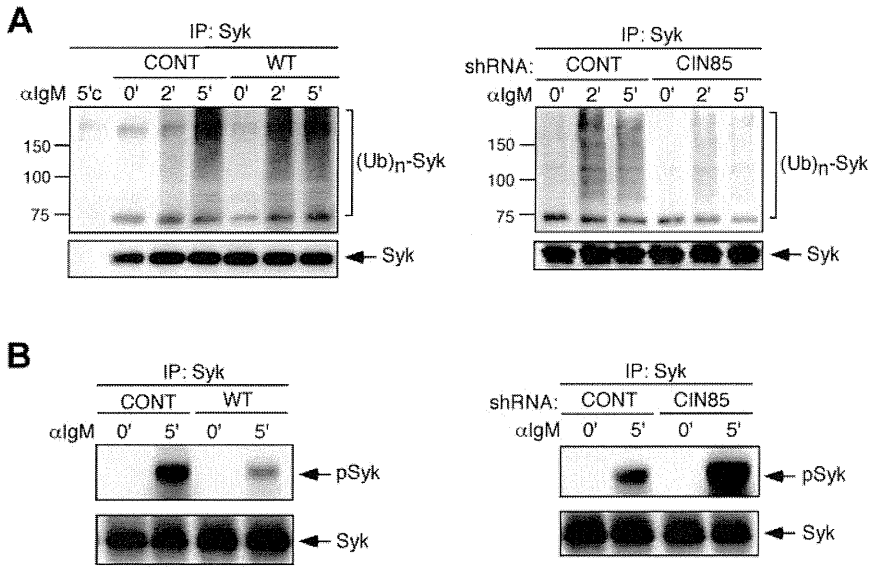

Figure 4. CIN85 promotes Syk ubiquitination and degradation in B cells. (A) Control BJAB cells, stable transformants expressing WT CIN85, and CIN85-knockdown BJAB cells were stimulated with 20 μg/mL $F(ab')_2$ goat anti–human IgM for the indicated time periods. Immunoprecipitates with anti-Syk mAb were separated on a 10% SDS-PAGE gel and analyzed by Western blotting with anti-ubiquitin or anti-Syk mAb. 5′′c, immunoprecipitation of the cell lysates at 5 minutes with isotype control. The molecular weight is indicated on the left side of the blots. (B) Control BJAB cells, stable transformants expressing WT CIN85, and CIN85-knockdown BJAB cells were stimulated with 20 μg/mL $F(ab')_2$ goat anti–human IgM for 5 minutes. Immunoprecipitates with anti-Syk mAb were separated on a 10% SDS-PAGE gel and analyzed by Western blotting with anti–phospho-Syk pAb or anti-Syk mAb.

whereas this induction was more pronounced in CIN85-knockdown B cells (Figure 6E). Consistent with the findings for the transcript levels, BCR stimulation alone did not induce detectable levels of Blimp-1 protein. However, the combined stimulation of BCR and TLR9 clearly induced the expression of the Blimp-1 protein in control cells, although this was more pronounced in CIN85-knockdown cells (Figure 6F). These results suggest that CIN85 is required for Cbl-mediated regulation of BCR signaling and downstream events such as the survival, growth, and differentiation of human B cells.

Discussion

We demonstrated here that CIN85 functions as a novel adaptor to regulate proximal BCR signaling. Gain-of-function and loss-of-function experiments revealed that CIN85 not only enhances BCR-induced c-Cbl phosphorylation but also inhibits BCR-induced calcium flux and the phosphorylation of Syk and PLCγ2. CIN85 promotes c-Cbl–dependent ubiquitination and degradation of Syk, which is a key upstream kinase that propagates BCR signaling by phosphorylating downstream molecules including PLCγ2. Because Cbl proteins directly associate with Syk and inhibit its function,[6] it is probable that CIN85 acts as a critical scaffolding adaptor for Cbl proteins and is indispensable for Cbl-mediated regulation of Syk activation in B cells.

Consistent with our findings, a critical role of CIN85 in Cbl-mediated regulation of Syk activation was recently shown in FcεRI signaling in mast cells.[21] In mast cells, CIN85 enhances c-Cbl-mediated ubiquitination and the degradation of Syk protein.[21] In B cells, however, CIN85 overexpression significantly increased Syk ubiquitination (Figure 4), but CIN85 knockdown did not alter the total levels of Syk protein throughout stimulation (Figure 3A), as previously shown in c-Cbl/Cbl-b double-knockout B cells.[10] This apparent discrepancy in Syk degradation between mast cells and B cells could be explained by the findings of Rao et al,[31] who showed that on BCR stimulation, only a small portion of Syk is phosphorylated and then degraded by c-Cbl. Rao et al also showed that c-Cbl does not directly affect the catalytic activity of Syk.[31] Consistent with these findings, our study showed that CIN85 promotes c-Cbl–mediated ubiquitination and degradation of the phosphorylated pool of Syk (Figure 4A-B).

What, then, are the possible mechanisms by which CIN85 enhances BCR-induced c-Cbl phosphorylation in B cells? Src-family PTKs and Syk are proposed to phosphorylate c-Cbl on tyrosines.[6] We previously showed that CIN85 directly interacts with the SH3 domain of Src-family PTKs including Lyn.[17] In addition, CIN85 directly associates with BLNK, PLCγ and Vav, all of which are direct Syk interactors,[17,36] and thus, CIN85 is indirectly associated with Syk via binding to BLNK, PLCγ, and Vav. In view of these findings, it seems probable that CIN85 acts as a key scaffolding adaptor that permits the spatial proximity of Src-family PTKs, Syk, and Cbl proteins and thus facilitates their phosphorylation of Cbl proteins.

Although CIN85 appears to function in concert with Cbl proteins to regulate BCR signaling, an additional mechanism is possible. Previous in vitro binding experiments showed that CIN85 directly binds to Src-family tyrosine kinases, PLCγ, p85 PI3K,Vav, Btk, and SHIP, all of which are involved in BCR signaling, through its SH3 domains and proline-rich region.[15,24,25] In addition, a recent study showed that the SH3 domains of CIN85 could uniquely bind to ubiquitin.[37] Thus, after various BCR-signaling molecules are ubiquitinated by Cbl proteins on stimulation, the competition between canonical SH3 ligands and ubiquitin binding to CIN85 may affect BCR signaling in a temporal and spatial manner. Therefore, it is probable that CIN85 also directly regulates BCR signaling by a Cbl-independent mechanism.

A recent study using liquid chromatography-coupled tandem mass spectrometry showed that 3 SH3 domains of CIN85 could recruit protein molecules required for the proper formation and

Figure 3 (continued) and CIN85-knockdown BJAB cells transfected with the NF-AT luciferase reporter construct were stimulated with graded doses of $F(ab')_2$ goat anti–human IgM for 8 hours and lysed, and the luciferase activity was assayed using a luminometer. The relative luciferase activity of the medium and BCR-stimulated cells was expressed with respect to that of the PMA/ionomycin stimulation. The results were presented as the mean and SEM of triplicate cultures. One experiment representative of 4 independent experiments is shown (*$P < .05$ vs controls). (G) Stable control and CIN85-knockdown BJAB cells before and after stimulation with 20 μg/mL $F(ab')_2$ goat anti–human IgM (3 and 5 hours) were analyzed for surface expression of CD69. One experiment representative of 3 independent experiments is shown (**$P < .01$ vs controls).

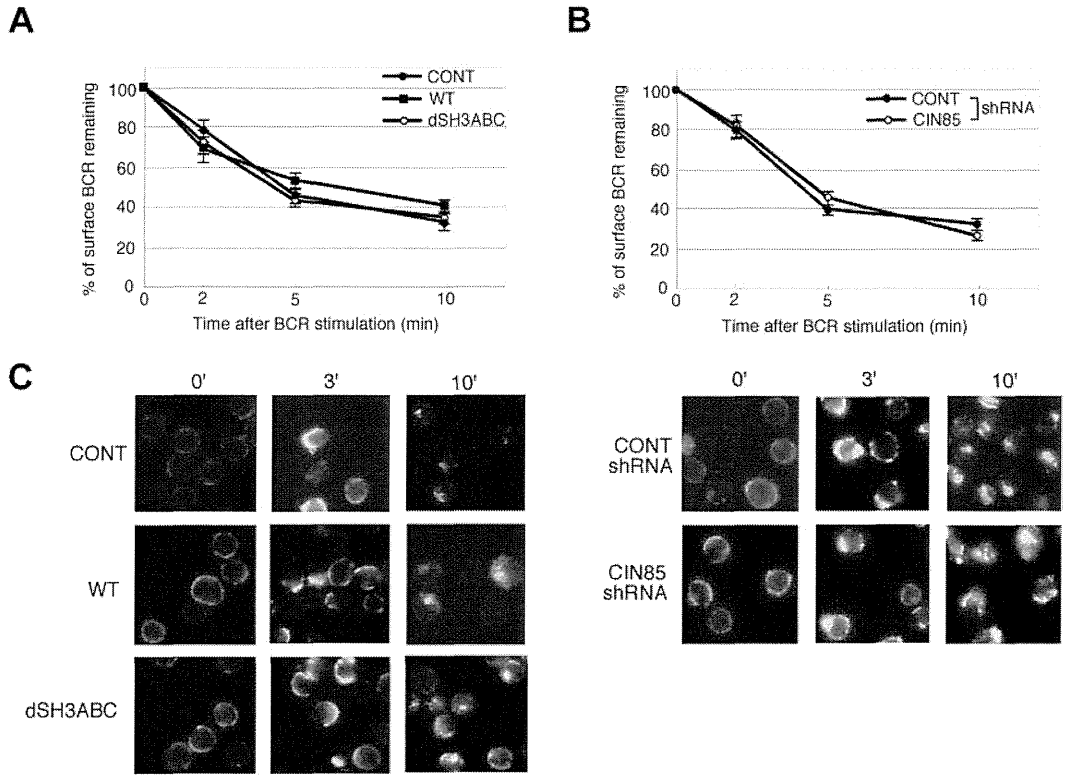

Figure 5. CIN85 does not affect BCR internalization. (A) BJAB cells (control and stable transformants expressing either WT or SH3-deleted CIN85) and (B) BJAB cells (control and CIN85-knockdown) were incubated at 4°C with $F(ab')_2$ goat anti–human IgM for 30 minutes. The cells were washed, warmed to 37°C for the indicated time intervals, stained at 4°C for 30 minutes with a FITC-labeled anti–goat IgG pAb, and analyzed by flow cytometry. The results are expressed as the percentage of surface BCRs remaining. The data are presented as the average and SEM of 3 independent experiments. (C) Control BJAB cells, stable transformants expressing either WT or SH3-deleted CIN85, and CIN85-knockdown BJAB cells were incubated at 4°C with 20 μg/mL $F(ab')_2$ goat anti–human IgM for 30 minutes. The cells were washed and warmed to 37°C for the indicated time periods. The cells were fixed, permeabilized, stained with a FITC-labeled anti–goat IgG pAb, and analyzed by fluorescence microscopy. The images shown are representative of 3 independent experiments.

function of coated vesicles.[25] Similarly, early studies showed a characteristic feature of CIN85 in the formation of clathrin-coated vesicles during the internalization of RTKs such as EGFRs in nonimmune cells.[18,19] Brain-specific CIN85-deficient mice manifest impaired internalization of D2 dopamine receptors, which belong to the 7-transmembrane G protein-coupled receptor superfamily.[38] In addition, CIN85 facilitates ligand-induced FcεRI internalization in RBL-2H3 mast cell lines.[20] Because BCR internalization is regulated via a clathrin-dependent pathway,[39] it was of interest to determine whether CIN85 regulates BCR internalization. Our study, however, shows that CIN85 does not affect BCR internalization (Figure 5, supplemental Figure 1). These data are somewhat surprising, given that Cbl proteins control BCR internalization by a ubiquitin-dependent mechanism.[10,40] However, the role of Cbl proteins in BCR ubiquitination and internalization is still rather controversial. The HECT family member Itch, but not c-Cbl, is an E3 ubiquitin ligase that is involved in BCR ubiquitination.[41] In addition, the ubiquitination of Igβ, which is a component of BCR, does not facilitate BCR internalization but is required for the sorting of early endosomes and for trafficking into late endosomes,[41] which suggests that BCR ubiquitination is more critical at the later stage of its trafficking. Because our imaging analysis (Figure 5C) cannot clearly distinguish the spatial distribution of early and late endosomes, it is of great interest to test whether CIN85 affects postendocytotic BCR trafficking. A recent study showed that in human neutrophils, CIN85 modulates c-Cbl–mediated down-regulation of FcγRIIa in the later stages of receptor trafficking without affecting the internalization of this receptor.[22]

During the submission of this paper, 2 studies were published that, in contrast to our findings, showed that CIN85 positively regulates BCR signaling in mouse and chicken B cells.[42,43] These studies found that CIN85 associates with BLNK and regulates BCR-induced NF-κB activation. However, the detailed profiles of BCR signaling differ between the 2 studies: the BCR-induced phosphorylation of BLNK and PLCγ2 and the calcium flux are significantly decreased on the loss of CIN85 in chicken B cells, whereas they are apparently normal in CIN85-deficient mouse B cells.[42,43] It should be noted that the former study did not actually use CIN85-deficient cells; rather, it used cells expressing a mutant BLNK that failed to bind to CIN85 or its homolog CD2AP.[42] Although these findings are intriguing, it is rather surprising that Cbl-mediated function of CIN85 in B cells was barely investigated in these studies. As previously mentioned, it is becoming evident that Cbl proteins play a critical role in the function of CIN85 in immune cells.[20-22] In addition, BCR-induced association of CIN85 with c-Cbl was recently shown even in mouse B cells.[44] We thus find that in human B cells, CIN85 negatively regulates BCR signaling via a Cbl-dependent mechanism. Our data obtained using CIN85-knockdown primary B cells also support this hypothesis. The molecular reason underlying the apparent discrepancy between our study and the aforementioned ones[42,43] remains unclear. One possibility, however, is that the relative contribution of CIN85-binding partners varies depending on the source of B cells used. In human B cells, Cbl proteins seem to preferentially associate with CIN85 over BLNK (Figure 1A). Notably, we found that CD2AP seems to preferentially associate with BLNK over c-Cbl in human B cells (supplemental Figure 2). It is therefore of potential interest

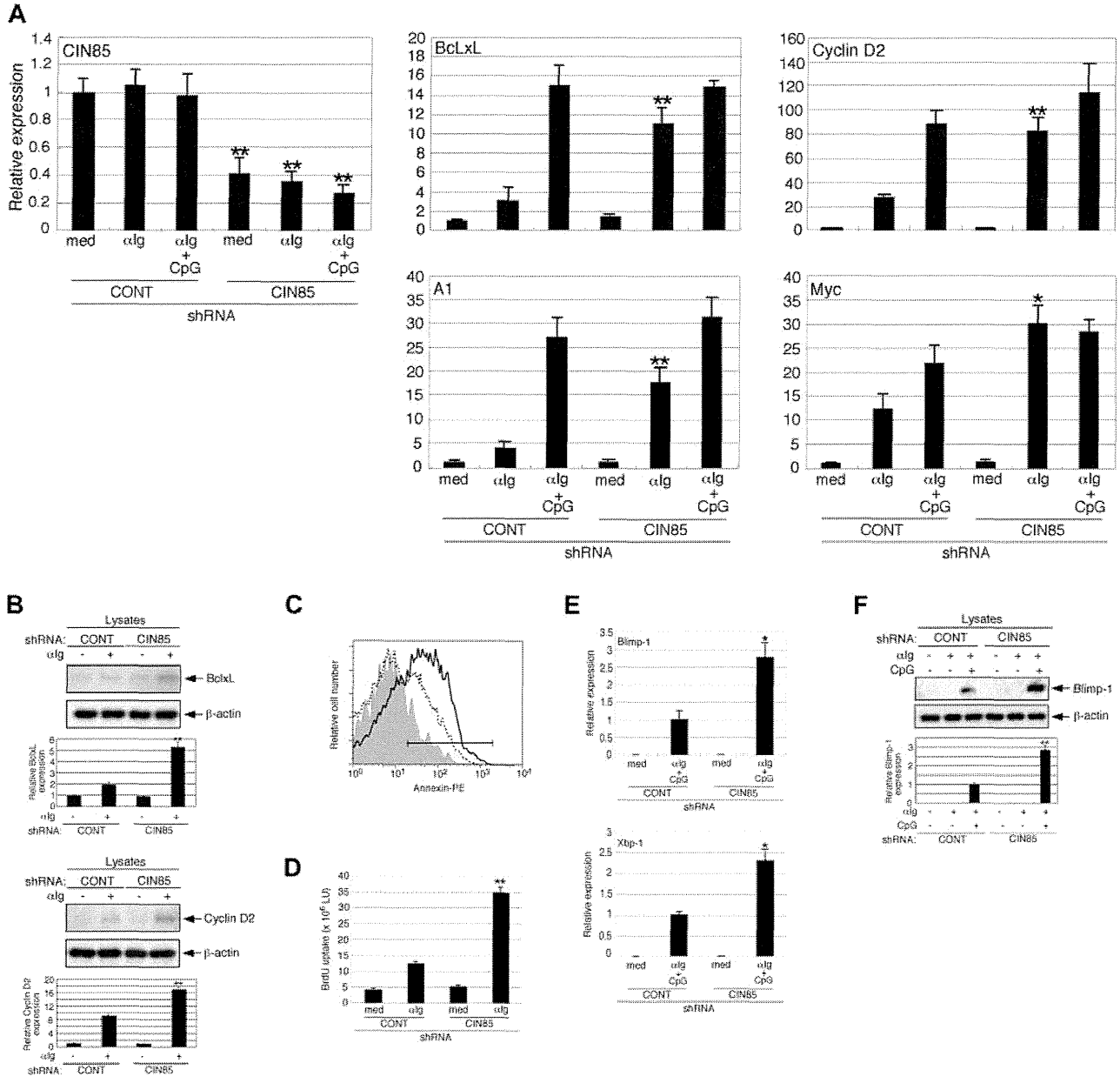

Figure 6. CIN85 knockdown enhances the survival, growth, and differentiation of primary B cells. (A) Control and CIN85-knockdown primary B cells were incubated for 24 hours in medium containing F(ab')$_2$ goat anti–human IgG/IgA/IgM (αIg, 20 μg/mL) or αIg plus CpG (1 μM), and CIN85, BcLxL, A1, cyclin D2, and myc mRNA levels were quantified by real-time PCR. The data are normalized to the expression of 18S rRNA. The results shown are representative of 3 independent experiments (*$P < .05$, **$P < .01$ vs controls). (B) Control and CIN85-knockdown primary B cells were incubated for 24 hours in the absence or presence of F(ab')$_2$ goat anti–human IgG/IgA/IgM (αIg, 20 μg/mL). The cell lysates were subsequently separated on a SDS-PAGE gel and analyzed by Western blotting with anti-BclxL mAb, anti-cyclin D2 pAb, or anti–β-actin mAb. The resulting values are expressed as fold changes in protein expression compared with nonstimulated control cells. The values are the mean ± SD of 3 independent experiments (**$P < .01$ vs controls). (C) Control and CIN85-knockdown primary B cells were incubated for 48 hours in the absence or presence of F(ab')$_2$ goat anti–human IgG/IgA/IgM (αIg, 20 μg/mL). After culture, the cells were stained with PE-labeled annexin V and analyzed using flow cytometry. The percentages of annexin-positive cells are shown. A representative histogram of 3 independent experiments is shown. (D) Control and CIN85-knockdown primary B cells were incubated for 48 hours in the absence or presence of F(ab')$_2$ goat anti–human IgG/IgA/IgM (αIg, 20 μg/mL). After culture, the cells were pulsed with BrdU, and its incorporation was detected by incubation with anti-BrdU mAb, followed by rhodamine-conjugated anti–mouse Ab. A representative histogram of 3 independent experiments is shown (**$P < .01$ vs controls). (E) Control and CIN85-knockdown primary B cells were incubated for 48 hours in the absence or presence of F(ab')$_2$ goat anti–human IgG/IgA/IgM (αIg, 20 μg/mL) and CpG (1 μM), and quantitation of Blimp-1 and Xbp-1 mRNA by real-time PCR was carried out. The data are normalized to the expression of 18S rRNA. The results shown are representative of 3 independent experiments (*$P < .05$ vs controls). (F) Control and CIN85-knockdown primary B cells were incubated for 48 hours with or without F(ab')$_2$ goat anti–human IgG/IgA/IgM (αIg, 20 μg/mL) in the absence or presence of CpG (1 μM). The cell lysates were subsequently separated on a SDS-PAGE gel and analyzed by Western blotting with anti–Blimp-1 mAb or anti–β-actin mAb. The resulting values are expressed as fold changes in protein expression compared with unstimulated control cells. The values are the mean ± SD of 3 independent experiments (**$P < .01$ vs controls).

to compare the roles of CIN85 and CD2AP in the function of human B cells.

BCR signals play a pivotal role in the survival, growth, and differentiation of B cells.[1,2] Under physiologic conditions, BCR signaling is fine-tuned by positive and negative regulators and is generally insufficient for the full activation of B cells, rendering them susceptible to apoptosis and anergy. However, when the negative regulation of BCR signaling is compromised, unwanted B cells could grow and survive, thereby potentially leading to autoimmunity and B-cell malignancies. This study showed that

CIN85 knockdown in primary B cells causes full activation of B cells and enhances BCR-induced survival and growth via the increased expression of BcLxL, A1, cyclin D2, and myc (Figure 6). Given that Cbl proteins are critical for B-cell anergy,[10] CIN85 may cooperate with Cbl proteins to function as a key negative regulator for BCR signaling and to maintain self-tolerance. It is thus of interest to determine whether the expression and/or function of CIN85 could be altered in human autoimmune diseases such as SLE. Surprisingly, CLL cells from advanced-stage patients exhibit hypophosphorylation of c-Cbl,[11] as seen in CIN85-knockdown cells. The manipulation of CIN85 expression may therefore provide a novel strategy to control aberrant cell growth and survival in B-cell malignancies.

Acknowledgments

The authors thank Editage for proofreading the English used in this paper.

This work was supported in part by a Grant-in-Aid from the Ministry of Education, Culture, Sports, Science, and Technology of Japan (H.N. and K.A.).

Authorship

Contribution: H.N. and K.A. designed and performed the research, analyzed the data, and wrote the paper; S.J.-T., Y.K., T.S., K.N., S.-i.O., H. Tsuzuki, Y.I., Y.A., H.I., S.S., E.B., H. Tsukamoto, and T.H. performed the research; and T.T. provided cDNA constructs and helped write the paper.

Conflict-of-interest disclosure: The authors declare no competing financial interests.

Correspondence: Hiroaki Niiro, Dept of Medicine and Biosystemic Science, Graduate School of Medical Sciences, Kyushu University, 3-1-1 Maidashi, Higashi-ku, Fukuoka 812-8582, Japan; e-mail: hniiro@med.kyushu-u.ac.jp.

References

1. Niiro H, Clark EA. Regulation of B-cell fate by antigen-receptor signals. *Nat Rev Immunol.* 2002;2(12):945-956.
2. Kurosaki T, Shinohara H, Baba Y. B cell signaling and fate decision. *Annu Rev Immunol.* 2010;28: 21-55.
3. Pogue SL, Kurosaki T, Bolen J, Herbst R. B cell antigen receptor-induced activation of Akt promotes B cell survival and is dependent on Syk kinase. *J Immunol.* 2000;165(3):1300-1306.
4. Thien CB, Langdon WY. c-Cbl and Cbl-b ubiquitin ligases: substrate diversity and the negative regulation of signalling responses. *Biochem J.* 2005; 391(pt 2):153-166.
5. Liu YC, Gu H. Cbl and Cbl-b in T-cell regulation. *Trends Immunol.* 2002;23(3):140-143.
6. Swaminathan G, Tsygankov AY. The Cbl family proteins: ring leaders in regulation of cell signaling. *J Cell Physiol.* 2006;209(1):21-43.
7. Duan L, Reddi AL, Ghosh A, Dimri M, Band H. The Cbl family and other ubiquitin ligases: destructive forces in control of antigen receptor signaling. *Immunity.* 2004;21(1):7-17.
8. Panchamoorthy G, Fukazawa T, Miyake S, et al. p120cbl is a major substrate of tyrosine phosphorylation upon B cell antigen receptor stimulation and interacts in vivo with Fyn and Syk tyrosine kinases, Grb2 and Shc adaptors, and the p85 subunit of phosphatidylinositol 3-kinase. *J Biol Chem.* 1996;271(6):3187-3194.
9. Yasuda T, Maeda A, Kurosaki M, et al. Cbl suppresses B cell receptor-mediated phospholipase C (PLC)-gamma2 activation by regulating B cell linker protein-PLC-gamma2 binding. *J Exp Med.* 2000;191(4):641-650.
10. Kitaura Y, Jang IK, Wang Y, et al. Control of the B cell-intrinsic tolerance programs by ubiquitin ligases Cbl and Cbl-b. *Immunity.* 2007;26(5):567-578.
11. Mankai A, Eveillard JR, Buhe V, et al. Is the c-Cbl proto-oncogene involved in chronic lymphocytic leukemia? *Ann N Y Acad Sci.* 2007;1107:193-205.
12. Niiro H, Maeda A, Kurosaki T, Clark EA. The B lymphocyte adaptor molecule of 32 kD (Bam32) regulates B cell antigen receptor signaling and cell survival. *J Exp Med.* 2002;195(1): 143-149.
13. Niiro H, Allam A, Stoddart A, Brodsky FM, Marshall AJ, Clark EA. The B lymphocyte adaptor molecule of 32 kilodaltons (Bam32) regulates B cell antigen receptor internalization. *J Immunol.* 2004;173(9):5601-5609.
14. Take H, Watanabe S, Takeda K, Yu ZX, Iwata N, Kajigaya S. Cloning and characterization of a novel adaptor protein, CIN85, that interacts with c-Cbl. *Biochem Biophys Res Commun.* 2000; 268(2):321-328.
15. Gout I, Middleton G, Adu J, et al. Negative regulation of PI 3-kinase by Ruk, a novel adaptor protein. *EMBO J.* 2000;19(15):4015-4025.
16. Bogler O, Furnari FB, Kindler-Roehrborn A, et al. SETA: a novel SH3 domain-containing adapter molecule associated with malignancy in astrocytes. *Neuro Oncol.* 2000;2(1):6-15.
17. Narita T, Amano F, Yoshizaki K, et al. Assignment of SH3KBP1 to human chromosome band Xp22.1–>p21.3 by in situ hybridization. *Cytogenet Cell Genet.* 2001;93(1-2):133-134.
18. Petrelli A, Gilestro GF, Lanzardo S, Comoglio PM, Migone N, Giordano S. The endophilin-CIN85-Cbl complex mediates ligand-dependent downregulation of c-Met. *Nature.* 2002;416(6877):187-190.
19. Soubeyran P, Kowanetz K, Szymkiewicz I, Langdon WY, Dikic I. Cbl-CIN85-endophilin complex mediates ligand-induced downregulation of EGF receptors. *Nature.* 2002;416(6877):183-187.
20. Molfetta R, Belleudi F, Peruzzi G, et al. CIN85 regulates the ligand-dependent endocytosis of the IgE receptor: a new molecular mechanism to dampen mast cell function. *J Immunol.* 2005; 175(7):4208-4216.
21. Peruzzi G, Molfetta R, Gasparrini F, et al. The adaptor molecule CIN85 regulates Syk tyrosine kinase level by activating the ubiquitin-proteasome degradation pathway. *J Immunol.* 2007;179(4):2089-2096.
22. Marois L, Vaillancourt M, Pare G, et al. CIN85 modulates the down-regulation of Fc gammaRIIa expression and function by c-Cbl in a PKC-dependent manner in human neutrophils. *J Biol Chem.* 2011;286(17):15073-15084.
23. Tabrizi SJ, Niiro H, Masui M, et al. T cell leukemia/lymphoma 1 and galectin-1 regulate survival/cell death pathways in human naive and IgM+ memory B cells through altering balances in Bcl-2 family proteins. *J Immunol.* 2009;182(3):1490-1499.
24. Narita T, Nishimura T, Yoshizaki K, Taniyama T. CIN85 associates with TNF receptor 1 via Src and modulates TNF-alpha-induced apoptosis. *Exp Cell Res.* 2005;304(1):256-264.
25. Havrylov S, Rzhepetskyy Y, Malinowska A, Drobot L, Redowicz MJ. Proteins recruited by SH3 domains of Ruk/CIN85 adaptor identified by LC-MS/MS. *Proteome Sci.* 2009;7:21.
26. Watanabe S, Take H, Takeda K, Yu ZX, Iwata N, Kajigaya S. Characterization of the CIN85 adaptor protein and identification of components involved in CIN85 complexes. *Biochem Biophys Res Commun.* 2000;278(1):167-174.
27. Chiu CW, Dalton M, Ishiai M, Kurosaki T, Chan AC. BLNK: molecular scaffolding through 'cis'-mediated organization of signaling proteins. *EMBO J.* 2002;21(23):6461-6472.
28. Marshall AJ, Niiro H, Yun TJ, Clark EA. Regulation of B-cell activation and differentiation by the phosphatidylinositol 3-kinase and phospholipase Cgamma pathway. *Immunol Rev.* 2000;176:30-46.
29. Turner M. B-cell development and antigen receptor signalling. *Biochem Soc Trans.* 2002;30(4): 812-815.
30. Peng SL, Gerth AJ, Ranger AM, Glimcher LH. NFATc1 and NFATc2 together control both T and B cell activation and differentiation. *Immunity.* 2001;14(1):13-20.
31. Rao N, Ghosh AK, Ota S, et al. The non-receptor tyrosine kinase Syk is a target of Cbl-mediated ubiquitylation upon B-cell receptor stimulation. *EMBO J.* 2001;20(24):7085-7095.
32. Sohn HW, Gu H, Pierce SK. Cbl-b negatively regulates B cell antigen receptor signaling in mature B cells through ubiquitination of the tyrosine kinase Syk. *J Exp Med.* 2003;197(11):1511-1524.
33. Su TT, Rawlings DJ. Transitional B lymphocyte subsets operate as distinct checkpoints in murine splenic B cell development. *J Immunol.* 2002; 168(5):2101-2110.
34. Yi AK, Chang M, Peckham DW, Krieg AM, Ashman RF. CpG oligodeoxyribonucleotides rescue mature spleen B cells from spontaneous apoptosis and promote cell cycle entry. *J Immunol.* 1998;160(12):5898-5906.
35. Calame KL, Lin KI, Tunyaplin C. Regulatory mechanisms that determine the development and function of plasma cells. *Annu Rev Immunol.* 2003;21:205-230.
36. Turner M, Schweighoffer E, Colucci F, Di Santo JP, Tybulewicz VL. Tyrosine kinase SYK: essential functions for immunoreceptor signalling. *Immunol Today.* 2000;21(3):148-154.

37. Stamenova SD, French ME, He Y, Francis SA, Kramer ZB, Hicke L. Ubiquitin binds to and regulates a subset of SH3 domains. *Mol Cell.* 2007; 25(2):273-284.

38. Shimokawa N, Haglund K, Holter SM, et al. CIN85 regulates dopamine receptor endocytosis and governs behaviour in mice. *EMBO J.* 2010; 29(14):2421-2432.

39. Stoddart A, Dykstra ML, Brown BK, Song W, Pierce SK, Brodsky FM. Lipid rafts unite signaling cascades with clathrin to regulate BCR internalization. *Immunity.* 2002;17(4):451-462.

40. Jacob M, Todd L, Sampson MF, Pure E. Dual role of Cbl links critical events in BCR endocytosis. *Int Immunol.* 2008;20(4):485-497.

41. Zhang M, Veselits M, O'Neill S, et al. Ubiquitinylation of Ig beta dictates the endocytic fate of the B cell antigen receptor. *J Immunol.* 2007;179(7): 4435-4443.

42. Oellerich T, Bremes V, Neumann K, et al. The B-cell antigen receptor signals through a preformed transducer module of SLP65 and CIN85. *EMBO J.* 2011;30(17):3620-3634.

43. Kometani K, Yamada T, Sasaki Y, et al. CIN85 drives B cell responses by linking BCR signals to the canonical NF-kappaB pathway. *J Exp Med.* 2011;208(7):1447-1457.

44. Buchse T, Horras N, Lenfert E, et al. CIN85 interacting proteins in B cells-specific role for SHIP-1. *Mol Cell Proteomics.* 2011;10(10):M110.

blood

2012 120: 3444-3454
Prepublished online August 30, 2012;
doi:10.1182/blood-2011-10-383240

Absence of LTB4/BLT1 axis facilitates generation of mouse GM-CSF–induced long-lasting antitumor immunologic memory by enhancing innate and adaptive immune systems

Yosuke Yokota, Hiroyuki Inoue, Yumiko Matsumura, Haruka Nabeta, Megumi Narusawa, Ayumi Watanabe, Chika Sakamoto, Yasuki Hijikata, Mutsunori Iga-Murahashi, Koichi Takayama, Fumiyuki Sasaki, Yoichi Nakanishi, Takehiko Yokomizo and Kenzaburo Tani

Blood (print ISSN 0006-4971, online ISSN 1528-0020), is published weekly by the American Society of Hematology, 2021 L St, NW, Suite 900, Washington DC 20036.

Absence of LTB4/BLT1 axis facilitates generation of mouse GM-CSF–induced long-lasting antitumor immunologic memory by enhancing innate and adaptive immune systems

*Yosuke Yokota,[1] *Hiroyuki Inoue,[1-3] Yumiko Matsumura,[1] Haruka Nabeta,[1] Megumi Narusawa,[1] Ayumi Watanabe,[1] Chika Sakamoto,[1] Yasuki Hijikata,[3] Mutsunori Iga-Murahashi,[3] Koichi Takayama,[2] Fumiyuki Sasaki,[4] Yoichi Nakanishi,[2] Takehiko Yokomizo,[4] and Kenzaburo Tani[1,3]

[1]Department of Molecular Genetics, Medical Institute of Bioregulation, Kyushu University, Fukuoka, Japan; [2]Research Institute for Diseases of the Chest, Graduate School of Medical Sciences, Kyushu University, Fukuoka, Japan; [3]Department of Advanced Cell and Molecular Therapy, Kyushu University Hospital, Kyushu University, Fukuoka, Japan; and [4]Department of Medical Biochemistry, Graduate School of Medical Sciences, Kyushu University, Fukuoka, Japan

BLT1 is a high-affinity receptor for leukotriene B4 (LTB4) that is a potent lipid chemoattractant for myeloid leukocytes. The role of LTB4/BLT1 axis in tumor immunology, including cytokine-based tumor vaccine, however, remains unknown. We here demonstrated that BLT1-deficient mice rejected subcutaneous tumor challenge of GM-CSF gene-transduced WEHI3B (WGM) leukemia cells (KO/WGM) and elicited robust antitumor responses against second tumor challenge with WEHI3B cells. During GM-CSF–induced tumor regression, the defective LTB4/BLT1 signaling significantly reduced tumor-infiltrating myeloid-derived suppressor cells, increased the maturation status of dendritic cells in tumor tissues, enhanced their CD4$^+$ T-cell stimulation capacity and migration rate of dendritic cells that had phagocytosed tumor-associated antigens into tumor-draining lymph nodes, suggesting a positive impact on GM-CSF–sensitized innate immunity. Furthermore, KO/WGM mice displayed activated adaptive immunity by attenuating regulatory CD4$^+$ T subsets and increasing numbers of Th17 and memory CD44^{hi}CD4$^+$ T subsets, both of which elicited superior antitumor effects as evidenced by adoptive cell transfer. In vivo depletion assays also revealed that CD4$^+$ T cells were the main effectors of the persistent antitumor immunity. Our data collectively underscore a negative role of LTB4/BLT1 signaling in effective generation and maintenance of GM-CSF–induced antitumor memory CD4$^+$ T cells. (*Blood.* 2012;120(17):3444-3454)

Introduction

For many cancers refractory to conventional therapies, gene-modified tumor vaccines have emerged as a promising treatment. Among numerous immunostimulatory cytokines used for tumor vaccines, GM-CSF has been the most intensively investigated and widely studied for use in clinical cancer vaccine trials.[1-3] Immunization with irradiated tumor cells engineered to secrete GM-CSF stimulates potent tumor-associated antigen (TAA)-specific antitumor immunity in preclinical[4,5] and clinical settings, including solid tumors and acute myeloid leukemia.[6,7] We have recently shown that the GM-CSF gene-transduced murine monocytic leukemia of WEHI3B cells lose their tumorigenicity when subcutaneously administered into wild-type (WT) BALB/c mice.[8] It is thought that the effective induction of antitumor immunity triggered by GM-CSF is mainly the result of augmented processing and presentation of TAAs by dendritic cells (DCs), followed by both CD4$^+$ and CD8$^+$ T-cell responses.[4,9,10] However, the efficacy of this therapy alone is not durable, partially because of its failure to maintain antitumor memory immunity by TAA-primed T cells. Therefore, there is an imminent need for elaborate studies to improve antitumor memory responses generated by GM-CSF gene-transduced tumor cells.

Leukotriene B4 (LTB4) is known to be an extremely potent lipid inflammatory mediator derived from membrane phospholipids by the sequential actions of 5-lipoxygenase and LTA4 hydrolase.[11] The major activities of LTB4 include the recruitment and activation of myeloid leukocytes, such as neutrophils.[12] Recently, Del Prete et al have reported a novel role of LTB4 in regulating migration of DCs that precede adaptive immune responses.[13] Lipid LTB4 mediates its functions through the G protein-coupled 7 transmembrane domain receptor superfamily,[14] namely, 2 distinct receptors, BLT1 and BLT2. On the other hand, GM-CSF stimulates the production and function of neutrophils, eosinophils, and monocytes, and activate maturation of DCs.[15,16] However, the underlying significance of the LTB4/BLT1 lipid chemo-attractant pathway in the field of tumor immunology, including GM-CSF-induced immunity, remains elusive.

In this context, we investigated the influence of the defective LTB4/BLT1 axis on antitumor memory responses induced by subcutaneous administration of WGM cells using WT and BLT1-knockout (KO) mice. Intriguingly, in vivo experiments showed that marked tumor rejection was reproduced only in BLT1-KO mice when WEHI3B cells were subcutaneously inoculated into WT or BLT1-KO mice that had rejected the outgrowth of WGM cells, implying that that the loss of the LTB4/BLT1 signaling may confer effective generation of TAA-specific memory T cells with retained antitumor effects triggered by GM-CSF. Therefore, the current

Submitted October 5, 2011; accepted August 13, 2012. Prepublished online as *Blood* First Edition paper, August 30, 2012; DOI 10.1182/blood-2011-10-383240.

*Y.Y. and H.I. contributed equally to this study.

The online version of this article contains a data supplement.

The publication costs of this article were defrayed in part by page charge payment. Therefore, and solely to indicate this fact, this article is hereby marked "advertisement" in accordance with 18 USC section 1734.

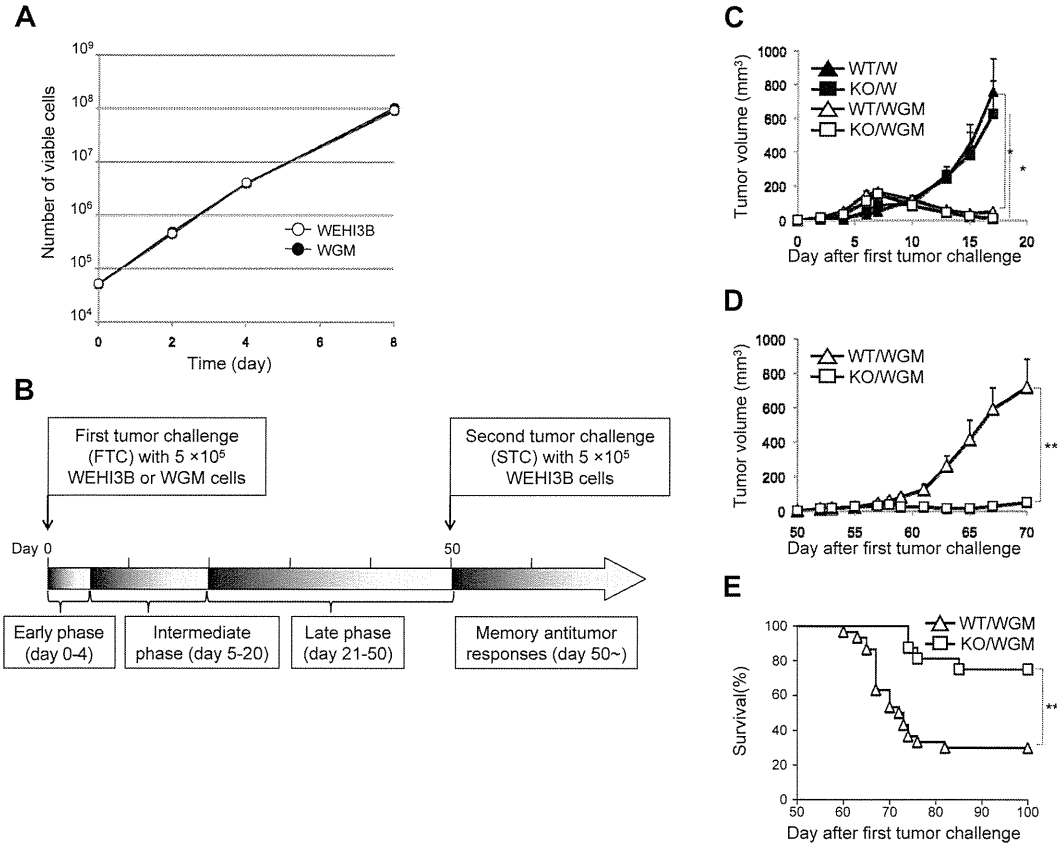

Figure 1. The absence of LTB4/BLT1 signaling induces potent antitumor effects against the second tumor challenge of WEHI3B cells after marked regression of WGM cells in mice model. (A) WEHI3B and WGM cells were cultured separately at 1 × 10^4 cells/well for 2, 4, 6, and 8 days in CM. At each time point, the number of viable cells was determined by trypan blue dye exclusion assay. (B) The explanatory scheme for all of the following in vivo experiments. The early phase, intermediate phase, and late phase in tumorigenicity assay are defined as spanning from days 0-4, 5-20, and 21-50 after the FTC, respectively. (C) In vivo tumorigenicity assay. The FTC consisted of 5 × 10^5 WEHI3B or WGM cells subcutaneously inoculated into the right flank of WT or BLT1-KO mice (n = 6–8). (D-E) In vivo STC assay. On day 50 after the FTC, 5 × 10^5 WEHI3B cells were subcutaneously inoculated into the left flank of mice that completely rejected the challenged tumor cells. The tumor volumes (mm^3) in 4 indicated mice groups were assessed on day 17. Kaplan-Meier survival curves are shown after the STC. Bars represent mean ± SEM. Significant difference: *$P < .05$, **$P < .01$. Representative data from 2-6 independent experiments with similar results are shown.

study explored the role of the LTB4/BLT1 signaling pathway in the induction of the persistent GM-CSF–induced antitumor memory responses.

Methods

Mice

BLT1-KO mice were established using a gene-targeting strategy, as previously described.[17] BLT1-KO mice and the corresponding WT mice have been backcrossed onto a BALB/c genetic background > 10 times. All animal experiments were carried out under the Guidelines for Animal Experiments of Kyushu University and Law 105 Notification 6 of the Japanese Government.

Tumor cells

WEHI3B cells obtained from Dr D. Metcalf (University of Melbourne) and recombinant mouse GM-CSF gene-transduced WEHI3B cell clones, established as previously described[18] were cultured in RPMI 1640 medium (Nacalai Tesque) supplemented with 10% heat-inactivated FBS and 1% penicillin-streptomycin solution (complete medium [CM]).

In vitro cell proliferation assay

WEHI3B and WGM cells were cultured independently in 48-well microplates at 5 × 10^4 cells/well for 2, 4, and 8 days in CM. On day 2, cells were transferred in 6-well plates and repeated every 2 days thereafter. The number of viable cells was determined by trypan blue dye exclusion assay (Invitrogen).

Tumor models

For the tumorigenicity assay, 5 × 10^5 cells/100 μL HBSS (Invitrogen) of WEHI3B cells or WGM cells were subcutaneously inoculated into the right flank of WT and BLT1-KO mice, respectively, as first tumor challenge (FTC; n = 6-8 per group). For the second tumor challenge (STC) assay, on day 50 after the subcutaneous inoculation of 5 × 10^5 cells of WEHI3B cells or WGM cells, 5 × 10^5 WEHI3B cells were subcutaneously inoculated into the left flank of mice that had completely rejected the challenged WEHI3B cells or WGM cells. Two bisecting diameters of each tumor were measured with calipers, and calculated using the formula $V = 0.4ab^2$, where "a" was the larger diameter and "b" was the smaller diameter of each tumor. Changes in tumor growth were monitored 3 times a week. Mice were killed for ethical reasons when the tumor diameter exceeded 15 mm. The explanatory scheme for all of the following in vivo experiments was illustrated in Figure 1B.

Analyses for tumor-infiltrating leukocytes

Approximately 5 × 10^6 WGM cells/100 μL were subcutaneously inoculated into the right flank of WT or BLT1-KO mice (n = 3-5 per group). One day after the FTC, the site of tumor inoculation was dissected as described previously.[5] Briefly, tumor tissue was finely minced and digested in RPMI 1640 containing collagenase (Invitrogen) for

20 minutes at 37°C, filtered through a 70-μm strainer, and washed in a fluorescent antibody buffer (FAB) consisting of 0.1% BSA in PBS. Supernatants from tumor tissue were collected, and homogenized cells were blocked with anti-FcR mAb for 15 minutes and followed by staining with either FITC– or PE/Cy7–anti-CD86, PE–anti-CD40, Alexa488– or peridinin-chlorophyll-protein (PerCP)–anti-CCR7, and allophycocyanin (APC)–anti-CD11c mAb either FITC–anti-CD11b, PE–anti-Gr-1, and APC–anti-F4/80, or FITC–anti-DX5, PE–anti-CD107a, and APC– or APC/Cy7–anti-CD3 mAb in FAB for 30 minutes, and subjected to multiparameter flow cytometry, a FACSCalibur or FACSVerse (BD Biosciences). Dead cells were excluded by 7-AAD staining and forward scatter/side scatter FSC/SCC profiles. Analyses of data were performed using FlowJo Version 8.8.6 software (Tree-Star). Concentrations of VEGF, TGF-β, and IL-10 in supernatants from tumor tissues were measured using Quantikine (R&D Systems) or mouse Th1/Th2 ELISA Ready-Set-Go (eBioscience).

MLR

One day after FTC, tumor-draining lymph nodes (TDLNs) and erythrocyte-depleted splenocytes were harvested from WT/WGM or KO/WGM mice as described in "Analyses for tumor-infiltrating leukocytes." DCs as stimulators (S) were purified from splenocytes or TDLNs using CD11c MicroBeads (Miltenyi Biotec). T cells as responders (R) were prepared from isolated splenocytes of C57BL/6 mice using Pan T cell isolation kit II (Miltenyi Biotec), suspended in CM supplemented with 50μM β-mercaptoethanol (Sigma-Aldrich), and cocultured with 30 Gy irradiated DCs at indicated R/T ratios on 96-well U-bottom plate for 4 days. Sixteen hours before the end of culture, 1 μCi [^{3}H]-thymidine (Moravek Biochemicals) was added to each well. Thymidine uptake was quantified in a TopCount NXT (PerkinElmer Life and Analytical Sciences). For CFSE-labeled mixed lymphocyte reaction (MLR) assay, splenic CD11c$^+$ DCs were isolated from WT/WGM or KO/WGM mice using CD11c MicroBeads (Miltenyi Biotec), irradiated with 30 Gy and cocultured with CD3$^+$ T cells as described in this section. After 6 days of coculture, the proliferation rate of CD3$^+$CD4$^+$ or CD3$^+$CD8$^+$ T cells labeled with 2.0μM CFSE (Invivogen) in the coculture was assessed by FACSVerse.

In vivo DC migration assay

Approximately 1×10^7 WGM cells were resuspended in 100 μL diluent C and incubated for 10 minutes with 1×10^{-6} M PKH26 (Sigma-Aldrich). After washing, 5×10^5 PKH26-labeled cells were subcutaneously inoculated into the right flank of WT and BLT1-KO mice. Two days after the FTC, TDLNs were homogenized by mechanical dissociation. Cell suspensions were pretreated with Fc-receptor (FcR) block and stained with FITC–anti-CD86 and APC–anti-CD11c mAb in FAB for 30 minutes. Cells were subjected to FACSCalibur or FACSVerse and analyzed using FlowJo Version 8.8.6 software.

Cytometric bead assay

Cytokine production profile from splenocytes was measured as previously described.[5] Briefly, 1 million splenocytes were harvested from WT or BLT1-KO mice challenged with WEHI3B cells or WGM cells on day 10, depleted of erythrocytes with ammonium chloride, and cocultured with or without 4×10^5 irradiated WEHI3B cells in CM for 20 hours. Production of IL-2, IL-4, IL-5, IFN-γ, and TNF-α in each supernatant was measured using Cytometric Bead Array mouse Th1/Th2 Cytokine kit (BD Biosciences), according to the manufacturer's instructions. Data were analyzed using FCAP Array Version 1.0.1 software (BD Biosciences).

Flow cytometric analysis for intracellular cytokines

On day 46 after the FTC, TDLNs or spleen were harvested from WT/WGM or KO/WGM mice (n = 3-5 per group). Homogenized cells were cultured in CM containing 50μM β-mercaptoethanol, phorbol myristate acetate (10 ng/mL), ionophore (250 mg/mL), and brefeldin A (1 ng/mL) for 4-5 hours. After washing, cells were pretreated with FcR block followed by staining with PerCP-anti–mouse CD4 mAb for 30 minutes. Subsequently, cells were fixed with 2% paraformaldehyde and stained intracellularly with FITC–anti-IFN-γ, PE–anti-IL-4, and APC–anti-IL-17A mAb in permeabilization buffer (eBioscience) for 30 minutes and subjected to FACSCalibur or FACSVerse.

Phenotypic analysis by flow cytometric analysis for diverse immune subpopulations

For mature DCs, TDLNs were harvested from the 4 groups of mice (n = 3 or 4 per group) on days 2 and 4 after the FTC. Obtained cells were blocked with FcR and stained with either FITC–anti-CD86, PE–anti-CD80, and APC–anti-CD11c mAb, or PE–anti-CD40 and APC–anti-CD11c mAb in FAB for 30 minutes. For diverse helper T subsets, TDLNs and splenocytes were harvested from WT/WGM or KO/WGM mice (n = 3-5 per group) on day 46 after the FTC. For memory T subsets, cells were stained with PE–anti-CD44, PerCP–anti-CD4, and APC–anti-CD62L mAb. For regulatory T cells, after staining with FITC–anti-CD3, PE–anti-CD25, and PerCP/Cy5.5–anti-CD4, TDLNs cells were resuspended with 100 μL Fixation/Permeabilization solution (BD Biosciences) and washed with BD Perm/Wash buffer (BD Biosciences) for 20 minutes, followed by the addition of APC–anti–FoxP3 (FJK-16; eBioscience) mAb, and incubated for 30 minutes. For other regulatory T cells, TDLNs and splenocytes were costained with FITC–anti-CD3, PE–anti-GITR, and PerCP–anti-CD4 mAb in FAB for 30 minutes, and subjected to FACSCalibur.

In vivo depletion experiments

GK1.5 and 2.43 hybridoma cells obtained from the Cell Resource Center for Biomedical Research (Institute of Development, Aging and Cancer Tohoku University) were used for the production of anti–mouse CD4 mAb and anti–mouse CD8 mAb, respectively, as previously described.[19] Briefly, these mAbs were purified with centrifugation at 53 000*g* for 20 minutes, and subjected to affinity chromatography using MAb Trap Kit (GE Healthcare). Effective depletion of CD4$^+$ and CD8$^+$ T cells was confirmed by flow cytometric analysis using splenocytes (data not shown). Mice received peritoneal injections of anti–mouse CD4 mAb, anti–mouse CD8 mAb (50 μg per mouse), or PBS for 3 days, and once every 3 days thereafter. For depletion of NK cells, mice received peritoneal injections of rabbit anti-asialo GM1 antiserum (diluted 1:20 in 200 μL PBS; Wako), on 1 day before the STC, and every 7 days thereafter.[20]

Adoptive T-cell transfer experiments

For Th17 adoptive cell transfer (ACT) therapy, Th17 cell preparation was performed as described previously[21] with minor modification. Briefly, splenic CD4$^+$ T cells from WT/WGM or KO/WGM mice on day 46 were magnetic cell sorting (MACS)-sorted using CD4$^+$T cell Isolation kit II(Miltenyi Biotec) and stimulated with plate-bound 1.0 μg/mL anti-CD3 (BD Biosciences) and 1.0 μg/mL anti-CD28 (BD Biosciences) under Th17 conditions with 1.0 ng/mL TGF-β (R&D Systems), 10 ng/mL IL-6 (R&D Systems), 5.0 μg/mL anti–IL-4 (clone 11B11), and 5.0 μg/mL anti–IFN-γ (clone XMG1.2). On day 4 after stimulation with phorbol myristate acetate and ionomycin, Th17 induction rate was confirmed to be ~ 65% among IL-17A–, IL-4–, or IFN-γ–producing T cells, and 1×10^6 cells were then intravenously injected into recipient syngeneic BALB/c mice. On the next day, they received subcutaneous challenge with 2×10^5 WEHI3B cells in the right flank. For CD4$^+$ T-cell ACT therapy, 5×10^5 splenic CD4$^+$CD44^{low} T or CD4$^+$CD44^{hi} T cells harvested from WT/WGM or KO/WGM mice were flow cytometrically (FACSAria, BD Biosciences)-sorted on day 3 after STC and injected intravenously into recipient syngeneic BLAB/c mice. They received subcutaneous challenge with 2×10^5 WEHI3B cells in the right flank.

Statistical analyses

The 2-tailed Student *t* test was used to evaluate *P* values between experimental groups. $P < .05$ was considered statistically significant.

Table 1. Comparison of the number of WGM cell-injected mice that rejected the second tumor challenge with WEHI3B cells between WT and BLT1-KO mice

	Mice that rejected first tumor challenge, no. (%)*	Mice that rejected second tumor challenge, no. (%)†
Female groups‡		
WT/WGM	30/35 (85.7)	9/30 (30.0)§
KO/WGM	16/16 (100)	13/16 (81.3)§
Male groups		
WT/WGM	0/6 (0)	—
KO/WGM	6/6 (100)	5/6 (83.3)§

— indicates not applicable.
*Assessed at day 50 after the first tumor challenge with WEHI3B or WGM cells.
†Assessed at day 50 after the second tumor challenge with WEHI3B cells.
‡Shown are combined pooled data from at least 3 independent experiments with similar results.
§χ^2 test ($P < .05$).

Survival was plotted using Kaplan-Meier curves, and statistical relevance was determined by a log-rank comparison using Prism 5 (GraphPad). All experiments were repeated at least twice.

Results

Absence of LTB4/BLT1 axis in GM-CSF–triggered immunity induces potent antitumor effects against secondary tumor challenge with WEHI3B cells

The GM-CSF production from WEHI3B cells was below detectable levels, whereas that from WGM cells was 136 ng/24 h/10^6 cells (supplemental Figure 1, available on the *Blood* Web site; see the Supplemental Materials link at the top of the online article) enough to induce substantial antitumor effects.[4,8] We compared in vitro proliferative ability between parental WEHI3B and WGM cells. Both cells exhibited an equal proliferation rate in a time-dependent manner (Figure 1A).

As myeloid cells, such as granulocytes, express abundant BLT1 and have direct antitumor effect,[22,23] we speculated that the magnitude of antitumor effect provoked by WGM cells would be attenuated when administered into BLT1-KO mice. To verify our speculation, WEHI3B cells or WGM cells (FTC) were subcutaneously inoculated into the right flank of female WT or BLT1-KO mice. WT mice challenged with WGM cells (WT/WGM mice) rejected tumor growth, whereas WT or BLT1-KO mice challenged with WEHI3B cells (WT/W or KO/W) died of tumor burden. Unexpectedly, BLT1-KO mice challenged with WGM cells (KO/WGM mice) also significantly rejected tumor growth ($P < .05$; Figure 1C). We next compared antitumor responses against secondary tumor challenge with WEHI3B cells long after the FTC rejection. On day 50 after the FTC, parental WEHI3B cells (STC) were subcutaneously inoculated into the opposite (left) flank of WT/WGM and KO/WGM mice that had completely rejected the FTC. Intriguingly, KO/WGM mice significantly again rejected the outgrowth of STC ($P < .01$; Figure 1D) and survived for significantly longer periods compared with WT/WGM mice ($P < .01$; Figure 1E; Table 1). Similar results were observed in experiments using male mice, showing no sexual difference in the STC-rejection mechanism (Table 1).

Previous studies have reported that LTB4 antagonists inhibit cell proliferation of several cancer cells.[24,25] To exclude the possibility that the rejection of STC was attributable to blocking of the LTB4/BLT1 axis-mediated direct antiproliferative effects, we examined BLT1 mRNA levels in WEHI3B and WGM cells by RT-PCR analysis. Both cells expressed undetectable levels of BLT1 mRNA (supplemental Figure 2), showing that the STC rejection was not induced by inhibition of LTB4/BLT1 signaling pathway.

Absence of LTB4/BLT1 axis facilitates activation of tumor-infiltrating innate immune subpopulations with mitigated immune tolerance in GM-CSF-induced antitumor immunity

We hypothesized that the rejection of STC could be induced by memory antitumor immunity. As GM-CSF–producing tumor cell vaccines not only induce the potent antitumor immunity by enhanced maturation of DCs[26] but also simultaneously recruit abundant immune-regulatory myeloid-derived suppressor cells (MDSCs),[27] we investigated the effect of blockade of LTB4/BLT1 signaling on tumor-infiltrating GM-CSF–sensitized diverse subsets of innate immune cells in early phase. The number of MDSCs and macrophages in tumors from KO/WGM mice were significantly decreased compared with those from WT/WGM mice ($P < .05$; Figure 2A-B). In contrast, the cell numbers of tumor-infiltrating NK cells, natural killer-like T cells (NKT), and cytolytic NK cells harvested from KO/WGM mice were significantly increased compared with those from WT/WGM mice (Figure 2C-E). In addition, the defective LTB4/BLT1 axis enhanced maturation of tumor-infiltrating DCs in tumors from KO/WGM mice compared with those from WT/WGM mice, as demonstrated by significantly increased expression of DC maturation markers, such as CD40 and CCR7 ($P < .05$; Figure 2F). Similar results were obtained for $CD86^+CD40^+$DCs, $CD40^+CCR7^+$DCs, $CCR7^+CD86^+$DCs, and $CD86^+CD40^+CCR7^+$DCs isolated from tumors ($P < .05$; Figure 2G-H). We subsequently compared the expression of the immune-regulatory cytokines VEGF, TGF-β, and IL-10 at the tumor injection site that might account for various DC maturation. Concentrations of VEGF, TGF-β, and IL-10 in the supernatants derived from single-cell suspensions of excised tumors from KO/WGM mice were significantly lower than those of WT/WGM mice ($P < .05$; Figure 2I). Lastly, to examine the effect of the defective LTB4/BLT1 axis on GM-CSF–primed DCs for T-cell activation, we performed MLR assay using allogeneic T cells from C57BL/6 mice and splenic- or TDLN-derived $CD11c^+$ DCs. The results showed that both splenic- (Figure 2J left panel) and TDLN- (Figure 2J right panel) derived DCs harvested from KO/WGM mice stimulated $CD3^+$ T cells more efficiently than those from WT/WGM mice. When we compared the stimulation capacity of DCs harvested from KO/WGM mice for $CD4^+$ and $CD8^+$ T cells, we observed a superior proliferation of $CD4^+$ T cells but not $CD8^+$ T cells (Figure 2K).

Absence of LTB4/BLT1 axis augments maturation and migration capacity of phagocytosed TAAs-DCs in GM-CSF-induced antitumor immunity

We next evaluated the impact of the defective LTB4/BLT1 axis on maturation of DCs in TDLNs on day 2 or 4 after FTC. As shown in Figure 3A-C and supplemental Figure 3, the mean fluorescence intensity of each CD40, CD80, and CD86 expression on DCs in TDLNs from KO/WGM mice was significantly more increased than that from WT/WGM mice ($P < .05$). To determine the influence of the defective LTB4/BLT1 axis on the migration

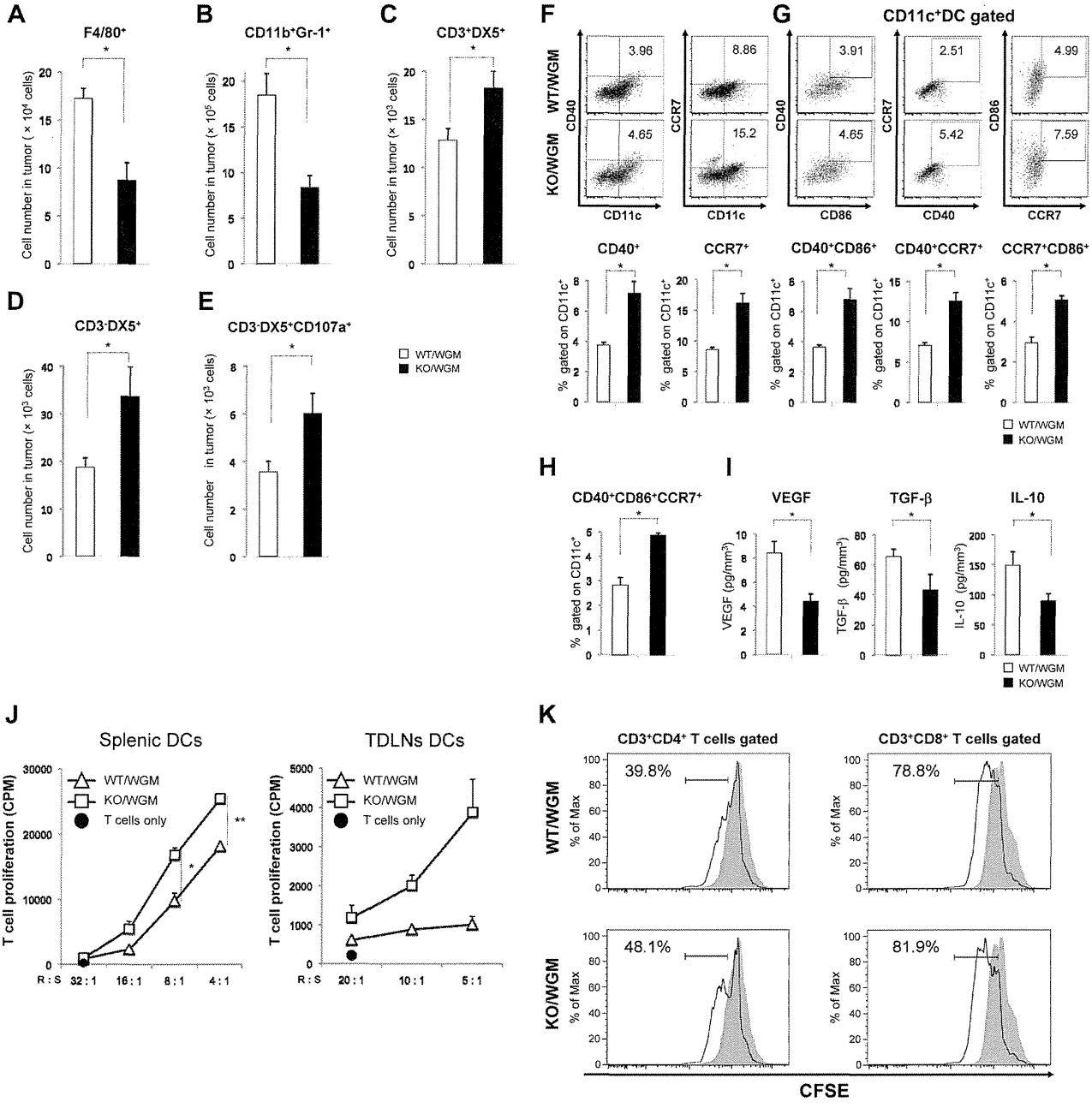

Figure 2. Absence of LTB4/BLT1 signaling promotes activation of various innate immune subpopulations in tumor tissues, accompanied with attenuated immune tolerance in KO/WGM mice. (A-E) One day after the FTC with WGM cells, tumors were excised from WT/WGM or KO/WGM mice, minced finely, and treated with collagenase for tissue dissociation. For assessment of innate immunity subpopulations, tumor infiltrating cells were subsequently analyzed by flow cytometry as described in "Analyses for tumor-infiltrating leukocytes." The numbers of viable cells are shown. (F-H) For detection of mature DCs, cells were stained with anti-CD11c, anti-CD40, anti-CD86, and anti-CCR7 mAb and subjected to flow cytometric analysis. Results shown are representative 2-dimensional dot plots (top panel, F-G) and bar graphs depicting the rates of indicated tumor infiltrating mature DCs (bottom panel, F-G). Numbers in 2-dimensional dot plots reflect the frequencies of (F) $CD40^+$ or $CCR7^+CD11c^+$cells, (G) $CD40^+CD86^+$, $CD40^+CCR7^+$, or $CCR7^+CD86^+CD11c^+$cells, and (H) $CD40^+CD86^+CCR7^+CD11c^+$ cells relative to the total $CD11c^+$ cells. (I) The concentrations of VEGF (n = 5 or 6), TGF-β (n = 3), and IL-10 (n = 9 or 10) in supernatants derived from smashed tumor tissue of WT/WGM or KO/WGM mice were measured by ELISA assay. (J) MLR assay evaluated by [^{3}H]thymidine incorporation. Various numbers of MACS-sorted splenic (left panel)- or TDLNs (right panel)-derived $CD11c^+$ DCs from WT/WGM or KO/WGM mice in early phase were 30 Gy irradiated as stimulator cells and incubated with 2×10^5 MACS-sorted splenic $CD3^+$ T cells (responder) harvested from splenic C57BL/6 mice at responder to stimulator (R:S) ratios as indicated for 4 days in triplicate. [^{3}H]Thymidine was added 16 hours before the cells were harvested, and thymidine incorporation was assessed using TopCount NXT microplate scintillation counter. Cultures in the absence of DCs (T cells only) were used as a negative control. (K) CFSE-labeled MLR assay. A total of 100 000 MACS-sorted splenic $CD11c^+$ DCs were harvested from WT/WGM or KO/WGM mice, irradiated with 30 Gy, and cocultured with $CD3^+$ T cells at an R:S ratio of 2:1. After 6 days of coculture, the proliferation rate of $CD3^+CD4^+$ T cells (left panel) or $CD3^+CD8^+$ T cells (right panel) labeled with 2.0μM CFSE in the coculture was assessed by flow cytometric analysis. The histograms are gated on $CD3^+CD4^+$ or $CD3^+CD8^+$ T cells. Cultures in the absence of DCs (T cells only) were used as a negative control. Bar graphs represent mean ± SEM. *Significant difference ($P < .05$). **Significant difference ($P < .01$). Representative data from 3 independent experiments or combined data from 2 independent experiments (D-E) with similar results are shown.

capacity of mature DCs that had engulfed TAAs into TDLNs, we compared a proportion of $CD86^+PKH26^+$ DCs in TDLNs between WT/WGM and KO/WGM mice on day 2 after the FTC. The frequency of $CD86^+PKH26^+$ DCs in TDLNs harvested from KO/WGM mice was > 5-fold higher than that from WT/WGM mice (Figure 3D).